Rearrangement of Proline Complexes with Zn<sup>2+</sup>: An Infrared Multiple Photon Dissociation and Theoretical Investigation

P. B. Armentrout,\*\*a Georgia C. Boles,\* Giel Berden,\* and Jos Oomens\*\*

<sup>a</sup>Department of Chemistry, University of Utah, 315 S. 1400 E. Rm. 2020, Salt Lake City, Utah 84112, United States

<sup>b</sup>Radboud University, Institute for Molecules and Materials, FELIX Laboratory, Toernooiveld 7, 6525 ED Nijmegen, The Netherlands

<sup>c</sup>van't Hoff Institute for Molecular Sciences, University of Amsterdam, Amsterdam, The Netherlands

\* Corresponding author, e-mail: armentrout@chem.utah.edu

Abstract: Complexes of proline (Pro) cationized with Zn<sup>2+</sup> and Cd<sup>2+</sup> were examined by infrared multiple photon dissociation (IRMPD) action spectroscopy using light generated from a free electron laser. Complexes of intact Pro with CdCl<sup>+</sup>, CdCl<sup>+</sup>(Pro), a complex of (Zn + Pro - H)<sup>+</sup> where a proton has been lost, as well as Zn<sup>+</sup>(Pro-H)(Pro) were formed by electrospray ionization. In order to identify the structures formed experimentally, the IRMPD spectra were compared to those calculated from optimized structures at the B3LYP/6-311+G(d,p) level for zinc complexes and B3LYP/def2-TZVP level with an effective core potential on cadmium for the CdCl<sup>+</sup>(Pro) system. For the latter complex, the main binding motif observed has a zwitterionic proline ligand structure, [CO2<sup>-</sup>]cc, where the metal binds to the two carboxylate oxygens. In contrast, for Zn<sup>+</sup>(Pro-H)(Pro), both ligands interact with zinc via a [N,CO<sup>-</sup>][N,CO] binding motif, where binding is observed at the carbonyl oxygens and nitrogens for both ligands, consistent with previous work. In both cases, contributions from different puckers of the proline ring may contribute. For (Zn+Pro-H)<sup>+</sup>, we identify that the structure is actually ZnH<sup>+</sup>(Pro-2H), in which the proline has been dehydrogenated and one of the hydrogens has migrated to form a covalent bond with Zn, which verifies a previous report relying on a single OH stretch band.

#### Introduction

The interactions of zinc with amino acids have been explored extensively in the gas phase. On the basis of low-energy collision-induced dissociation (CID) experiments and computations, Rogalewicz, Hoppilliard, and Ohanessian concluded that, in solution, complexes of deprotonated glycine (Gly-H)<sup>-</sup> with Zn<sup>2+</sup>, (Zn+Gly-H)<sup>+</sup>, had a [N,CO<sup>-</sup>] structure in which Zn binds to the amine nitrogen and a carboxylate oxygen. However, upon electrospray ionization, during the last desolvation step, these complexes had rearranged to a [N-,CO] structure as well as to ZnH<sup>+</sup>(Gly-2H), in which a hydrogen atom had migrated to form a covalent bond with Zn forming a much lower energy species according to calculations. Calculations were also used to show that these rearrangements are lower energy processes than desolvation from the solvated (CH<sub>3</sub>OH)Zn<sup>+</sup>(Gly-H) complex.<sup>2</sup> Further work showed that the ZnH<sup>+</sup>(Gly-2H) species must be formed during the electrospray process and is not present in solution.<sup>3</sup> These authors extended their studies to zinc complexes of other solvents (from water/methanol to water/acetonitrile) and other amino acids.<sup>4</sup> When (Zn+Gly-H)<sup>+</sup> was formed from either of these solvent mixtures, the distribution of structures differed (dependent on the cone voltage), but rearrangement was always observed. For other amino acids, they found that complexes of Zn<sup>2+</sup> with deprotonated serine (Ser), threonine (Thr), glutamine (Gln), histidine (His), and methionine (Met) showed no evidence for rearrangements, whereas the Zn<sup>+</sup>(Xxx-H) complexes of aspartic acid (Asp) and asparagine (Asn) showed different fragmentation patterns when electrosprayed from water/methanol versus water/acetonitrile. These results were interpreted to indicate more substantial rearrangement to a ZnH<sup>+</sup> structure when the more strongly binding acetonitrile ligand was present compared to methanol. These authors concluded that rearrangement could be favored depending on the strength of the solvent binding (weak for methanol and stronger for acetonitrile).

Interestingly, a non-rearranged zinc glycine complex has been observed.<sup>5</sup> When a Zn<sup>+</sup>(Thr-H)(CH<sub>3</sub>CN) complex was irradiated by a CO<sub>2</sub> laser, it preferentially lost acetaldehyde, the Thr side chain, rather than losing the acetonitrile ligand. This yielded Zn<sup>+</sup>(Gly-H)(CH<sub>3</sub>CN), which was interrogated using infrared multiple photon dissociation (IRMPD) spectroscopy and ab

initio theory. The structure consistent with the observed spectrum exhibited no hydrogen migration and retains the deprotonated glycine structure with coordination to a carboxylate oxygen atom and the amine nitrogen, the [N,CO<sup>-</sup>] structure.

Further IRMPD spectroscopy studies in combination with theory have provided more direct structural information regarding the complexes of zinc with various amino acids. Here, electrosprayed complexes of deprotonated His with both zinc and its congener cadmium, formed M<sup>+</sup>(His-H) complexes in which the metal is tridentate coordinated with the amine nitrogen, the deprotonated oxygen of the carboxylate group, and the pros  $(\pi)$  nitrogen of the histidine side chain (SC), referred to as [N,CO-,SC] coordination. Similar [N,CO-,SC] coordination has been observed for zinc complexed with deprotonated Gln, arginine (Arg), lysine (Lys), and Met, 10 whereas cysteine (Cys) deprotonates at the sulfur side-chain heteroatom, [N,CO,SC-]. 11 Ser, 12 Thr,<sup>5</sup> glutamic acid (Glu),<sup>13</sup> Asp,<sup>14</sup> and Met<sup>10</sup> show [N,CO<sup>-</sup>,SC] complexation in Zn<sup>+</sup>(Xxx-H)(CH<sub>3</sub>CN) complexes, with Ser and Thr also exhibiting [N,CO,SC<sup>-</sup>] coordination. In all these cases, no rearrangement to a ZnH<sup>+</sup>(Xxx-2H) species was observed, which we speculate may be because the internal solvation afforded by the side chain interaction or polar solvent molecule interferes with the hydrogen migration. For Asp, we found that the "expected" Zn<sup>+</sup>(Asp-H) [N,CO<sup>-</sup> ,SC] complex was a very minor contributor to the observed spectrum and instead the molecule had rearranged to expel ammonia, yielding (NH<sub>3</sub>)Zn<sup>+</sup>(Asp-NH<sub>4</sub>)[CO<sub>2</sub><sup>-</sup>,SC], where the zinc is fourcoordinate. 14 This prompted a reexamination of previous results for the related (Zn+Asn-H)+, which had originally been assigned as the [N,CO-,SC] structure, 15 but which upon further examination had an appreciable amount of the similarly rearranged (NH<sub>3</sub>)Zn<sup>+</sup>(Asn-NH<sub>4</sub>) complex. 14 These variations are consistent with the more general observations of Ohanessian and co-workers.<sup>4</sup> Finally, for the three aromatic amino acids, phenylalanine (Phe), tyrosine (Tyr), and tryptophan (Trp), only ZnCl<sup>+</sup>(Xxx) and CdCl<sup>+</sup>(Xxx) species were formed and all had [N,CO,SC] coordination.<sup>16</sup>

If the hypothesis that side chain interactions can inhibit hydrogen migration in zinc amino acid complexes, then proline should behave much like glycine. Indeed, Gholami and Fridgen

concluded that deprotonated proline complexed with zinc has the rearranged ZnH<sup>+</sup>(Pro-2H) structure as ascertained on the basis of CID experiments as well as the observation of a single IR band at 3557 cm<sup>-1</sup> associated with an OH stretch.<sup>17</sup> Computations indicated such a band could be consistent with ZnH<sup>+</sup>(Pro-2H), where proline is dehydrogenated at the nitrogen along with either C5 or C2 carbons of the ring, or a Zn<sup>+</sup>(Pro-H) deprotonated at the nitrogen and complexed as [N<sup>-</sup>,CO]. Additional experiments on the Zn<sup>+</sup>(Pro-H)(Pro) complex suggested that this species had not rearranged and likely had an [N,CO<sup>-</sup>][N,CO] coordination largely on the basis of computations.<sup>18</sup> Interestingly, this complex dissociated primarily by dehydrogenation (up to two times) upon IR irradiation, whereas loss of Pro dominated under SORI/CID conditions. This study was later extended to the complexes of (Pro-H)(Pro) with other metal dications (Mg, Ca, Sr, Ba, Mn, Fe, Co, Ni, Cu).<sup>19</sup>

In order to more definitively determine the conformations of the (Zn+Pro-H)<sup>+</sup> and Zn<sup>+</sup>(Pro-H)(Pro) isomers, the present study utilized IRMPD spectroscopy to interrogate these species in the fingerprint region between 600 and 1850 cm<sup>-1</sup>. As in many of our past studies of zinc amino acid complexes,<sup>5-16</sup> we also include cadmium in order to explore whether this metal, toxic because it can replace zinc in biological systems, yields different complexation. In all cases, IRMPD action spectra were compared to spectra calculated for a series of low-energy conformers with optimized structures and vibrational frequencies determined at the B3LYP/6-311+G(d,p) level for zinc complexes and B3LYP/def2-TZVP level of theory for cadmium complexes, where an SDD effective core potential (small core) was used for cadmium. Comparison of the calculated and experimental spectra of each system allows for clear identification of the experimentally generated complexes.

#### **Experimental and Computational Section**

Mass Spectrometry and Photodissociation. Experiments were performed using a 4.7 T Fourier transform ion cyclotron resonance (FT-ICR) mass spectrometer that was located at the Free Electron Lasers for Infrared experiments (FELIX) facility, Radboud University, The

Netherlands.<sup>20</sup> The FT-ICR has been described previously.<sup>21-23</sup> Ions of interest were generated using a Micromass Z-Spray electrospray ionization (ESI) source. They were accumulated in a hexapole trap for  $\sim$ 5 s, pulse extracted through a quadrupole bender, transported to the ICR cell via a radiofrequency (rf) octopole ion guide, and then injected. Collisional heating of the ions was avoided by electrostatic switching of the dc bias on the octopole.<sup>22</sup> Once the ions were trapped in the ICR cell, they were mass selected using a stored waveform inverse Fourier transform (SWIFT) excitation pulse.<sup>24-25</sup> These ions (presumed to be nearly room temperature) were irradiated using the FEL-2 beam line for 2 – 3 s at a 10 Hz macropulse repetition rate (energy up to 80 mJ per macropulse and a bandwidth of 0.5% of the central frequency).

Metalated Pro complexes were prepared from solutions of ~1.0 mM Pro and ~1.0 mM  $Zn(NO_3)_2$  or  $CdCl_2$  in 60:40 MeOH/H<sub>2</sub>O solvent. Flow rates of ~6  $\mu$ L/min were used, and the ESI needle was held at a voltage of 2.9 kV. For Zn, three complexes were generated,  $(Zn+Pro-H)^+$ , in which proline is deprotonated,  $(Zn+Pro+H)^+$ , and  $Zn^+(Pro-H)(Pro)$ . Relative amounts of the  $(Zn+Pro-H)^+$  and  $(Zn+Pro+H)^+$  were sensitive to the source conditions, but no conditions that isolated one or the other species could be located. Although the signals for these two species nearly overlap at m/z 180 and 182 because of zinc isotopes at m/z 64, 66, and 68, the high resolution of the FTICR can distinguish the two species. These are separated by an amount that is consistent with a difference of two hydrogen atoms at 1.0078 Da each and the difference in the Zn isotopes, for a total mass difference of about 0.015 Da. For Cd, the only relevant complex formed retained the chloride ligand, yielding CdCl<sup>+</sup>(Pro). In all cases, the resulting ions were mass isolated, allowed to cool radiatively for 0.4 s,<sup>26</sup> and then irradiated with the output of the free electron laser. To enhance the FEL-induced dissociation of  $(Zn+Pro-H)^+$  and CdCl<sup>+</sup>(Pro), the ions were irradiated for 50 and 30 ms, respectively, with a 30-W continuous-wave CO<sub>2</sub> laser directly after each FEL pulse.

Experimental IRMPD spectra were generated by calculating the photofragmentation yield,  $Y = \sum I_F / (\sum I_P + \sum I_F)$ , where  $I_P$  and  $I_F$  are the integrated intensities of the parent and fragment ion mass peaks as a function of the frequency of IR radiation. The photofragmentation yields were

linearly corrected for frequency dependent variation in the laser pulse energy. The application of a linear laser power correction is well described in the literature.<sup>27</sup>

Computational Details. In order to determine low-lying conformers of the cationized Pro complexes, conformers of Pro were first optimized at the B3LYP/6-311+G(d,p) level, using the Gaussian 09 suite of programs.<sup>28</sup> For the zinc system with one proline, each of these structures were deprotonated at all possible sites, and a Zn<sup>2+</sup> dication was added at all reasonable binding sites. Previous work on the (Zn+Pro-H)<sup>+</sup> complex<sup>17</sup> also suggested that ZnH<sup>+</sup>(Pro-2H) was formed, hence loss of a hydrogen atom from the already deprotonated proline ligand at multiple sites was also explored. For the Zn<sup>+</sup>(Pro-H)(Pro) complex, a more limited conformational search was conducted because many structural variations have already been explored in the literature. <sup>18</sup> Only the lowest-energy conformational motif was examined here for comparison to the IRMPD spectrum. For the cadmium systems, CdCl<sup>+</sup> was added to Pro at all possible binding sites. In all cases, the pucker associated with the five-membered proline ring was explicitly explored. Initial optimizations of the metalated complexes were then done using the "loose" keyword to utilize a large step size of 0.01 au and an rms force constant of 0.0017 to facilitate convergence. Unique structures were then further optimized at the B3LYP/6-311+G(d,p) level of theory for Zn<sup>2+</sup> complexes. For cadmium complexes, geometries were optimized at the B3LYP/def2-TZVP level, where def2-TZVP is a size-consistent basis set for all atoms and includes triple- $\zeta$  + polarization functions with a small-core (28 electron) effective core potential (ECP) on Cd. <sup>29-30</sup> The def2-TZVP basis set and corresponding ECP were obtained from the Basis Set Exchange.<sup>31</sup> These levels of theory, basis sets, and ECP have previously proven to provide accurate structural information with complexes of similar size and composition.<sup>5-16</sup>

Vibrational frequencies were scaled by 0.975 in the calculation of predicted spectra for comparison to the IRMPD spectra. This scaling factor accurately accounts for known inaccuracies in the calculated frequencies and their anharmonicities, and therefore gives good agreement with well-resolved bands in IRMPD spectra of other zinc and cadmium amino acid complexes.<sup>5-16</sup> When comparing to the experimental IRMPD spectra, calculated frequencies were broadened

using a 25 cm<sup>-1</sup> full-width at half maximum Gaussian line shape, which accounts for the finite laser bandwidth, unresolved rotational structure of the ions (which are near room temperature), and multiple photon effects.<sup>32</sup> When comparing experimental and theoretical IR spectra, it should be remembered that the experimental multiple photon intensities may not always be reproduced by the calculated one-photon linear absorption spectrum. Nevertheless, IR spectra obtained using IRMPD methods are generally comparable to those recorded using linear absorption techniques, in part because the spectra result from incoherent, rather than coherent, multiple photon excitation. This near-linear absorption character of IRMPD spectra has been demonstrated in previous modeling studies.<sup>32-33</sup>

Relative energies were determined using single point energies calculated at the B3LYP, B3P86, and MP2(full) levels using 6-311+G(2d,2p) (Zn<sup>2+</sup> complexes) and def2-TZVPP (Cd<sup>2+</sup> complexes) basis sets using the B3LYP geometries. Using vibrational frequencies scaled by 0.989, single point energies were adjusted to 0 K relative enthalpies by applying zero point energy (ZPE) corrections. Likewise, 298 K Gibbs energies were calculated as outlined previously from 0 K relative enthalpies by using the rigid rotor/harmonic oscillator approximation with the calculated rotational constants and vibrational frequencies.<sup>34</sup>

## **Results and Discussion**

**IRMPD Action Spectroscopy.** IRMPD action spectra were measured for CdCl<sup>+</sup>(Pro), Zn<sup>+</sup>(Pro-H)(Pro), and (Zn+Pro-H)<sup>+</sup> complexes over the range of 5.4 to 16.7 μm (600 – 1850 cm<sup>-1</sup>). The IRMPD of CdCl<sup>+</sup>(Pro) resulted in only one major fragment, as shown in reaction 1,

$$CdCl^{+}(Pro) [m/z 264] + n hv \rightarrow (Pro-H)^{+} [m/z 114] + HCdCl$$
 (1)

indicating that the fragment ion does not contain either Cd or Cl. Reactant masses monitored included m/z 260, 261, 262, 263, 264, and 266. The most abundant isotopes of Cd and Cl,  $^{114}$ Cd (28.73 %) and  $^{35}$ Cl (75.78 %), would form the complex at m/z 264, so the remaining peaks include isotopes  $^{113}$ Cd (12.22 %),  $^{112}$ Cd (24.13 %),  $^{111}$ Cd (12.80 %),  $^{110}$ Cd (12.49 %), and  $^{37}$ Cl (24.22 %). It seems feasible that the neutral product might also be Cd + HCl.

For the Zn<sup>+</sup>(Pro-H)(Pro) complex, all three zinc isotopes ( $^{64}$ Zn, 49.17% natural abundance;  $^{66}$ Zn 27.73%;  $^{68}$ Zn, 18.45%) $^{35}$  were monitored as the reactant ion: m/z 293, 295, 297. Fragmentations included reactions 2, in agreement with previous results of Gholami and Fridgen. $^{18}$  The fragment masses shown were all monitored and included in the yield calculation as was m/z 180, presumed here to be mainly the  $^{66}$ Zn isotope of the (Zn+Pro-H)<sup>+</sup> product.

$$^{64}\text{Zn}^{+}(\text{Pro-H})(\text{Pro}) [m/z \ 293] + \text{n hv} \rightarrow (^{64}\text{Zn}+\text{Pro-H})^{+} [m/z \ 178] + \text{Pro}$$
 (2a)

$$\rightarrow$$
 (Pro+H)<sup>+</sup> [m/z 116] + <sup>64</sup>Zn + (Pro-2H) (2b)

$$\rightarrow (C_4H_8N)^+[m/z 70] + CO + H_2O + {}^{64}Zn + (Pro-2H)$$
 (2c)

$$\rightarrow (^{64}\text{Zn+Pro+H})^{+} [m/z \ 180] + (\text{Pro-2H})$$
 (2d)

Notably, by isolating the m/z 293 ( $^{64}$ Zn) species, Gholami and Fridgen found that IRMPD and sustained off-resonance irradiation (SORI) CID of Zn<sup>+</sup>(Pro-H)(Pro) also led to H<sub>2</sub> loss, as verified by deuterium labeling experiments. Further, this ion also produced m/z 180, indicating a contribution from ( $^{64}$ Zn+Pro+H)<sup>+</sup>, reaction 2d. Indeed, in the present work, a high resolution FTICR scan of the m/z 180 product indicated two species separated by a difference consistent with two hydrogen atoms and the zinc isotopes, i.e., both ( $^{66}$ Zn+Pro-H)<sup>+</sup> and ( $^{64}$ Zn+Pro+H)<sup>+</sup> were observed. In our experiments, the former ion must have come from the analogue of reaction 2a with the  $^{66}$ Zn(Pro-H)(Pro) isotopic precursor. Unfortunately, at the time of these experiments, the extra (Zn+Pro+H)<sup>+</sup> peaks were an unidentified contaminant, hence no spectra related to this species was obtained.

IRMPD of the (Zn+Pro-H)<sup>+</sup> complex resulted in the fragmentations shown in reactions 3.

$$(^{64}\text{Zn+Pro-H})^+[m/z \ 178] + \text{n hv} \rightarrow (\text{Pro-H})^+[m/z \ 114] + ^{64}\text{Zn}$$
 (3a)

$$\rightarrow (C_4H_6N)^+[m/z 68] + CO + H_2O + {}^{64}Zn$$
 (3b)

The mass to charge ratio of the ion shown here uses the mass of <sup>64</sup>Zn, the most abundant isotope. Channels corresponding to <sup>66</sup>Zn and <sup>68</sup>Zn were *not* included in the yield calculation because these overlap with the (Zn+Pro+H)<sup>+</sup> species also formed.

These dissociation results agree with those previously observed using SORI-CID by Gholami and Fridgen. <sup>17</sup> These authors also observed additional minor channels corresponding to losses of  $H_2O$ , CO,  $CO_2$ , and  $Zn + H_2O$ .

**Nomenclature.** Here, complexes are identified using nomenclature outlined previously,<sup>36</sup> in which complexes are designated by the metal binding sites in square brackets. The deprotonation or dehydrogenation sites (if present) are indicated by a negative sign and the atoms having lost hydrogen. When needed, the designation of the metal binding site is followed by the amino acid orientation, which is represented by the characterization of  $\angle$ NCCO and  $\angle$ CCOH dihedral angles as cis (c, for angles between 0° and 45°), gauche (g, 45° - 135°), or trans (t, 135° - 180°).

For the ZnH<sup>+</sup>(Pro-2H) complexes where a hydrogen has migrated from deprotonated proline to zinc, the site where the hydrogens have been lost are designated after the metal binding sites, e.g., [N,CO]-N,C2, where C2 designates the carbon attached to the carboxylic acid. In one case, [CO]-C3,C4,ZW, the hydrogens have been removed from the C3 and C4 positions but the hydrogen on the carboxylic acid group has also migrated to the nitrogen forming a zwitterionic (ZW) ligand.

Because of the five-membered ring of proline, the pucker in this ring can also vary. This is designated in the standard way as the carbon (or nitrogen) furthest from the plane of the other four atoms in the ring. When tilted towards the carboxylic acid or carboxylate, the pucker is called "endo" and when tilted away, it is called "exo". In cases where the pucker is not explicitly noted, alternative possibilities were verified to collapse to the designated structure.

For the Zn<sup>+</sup>(Pro-H)(Pro) complexes, orientations of two stereocenters are also designated as R or S. In the low-energy conformers located, the two ligands form a pseudo-tetrahedral complexation geometry with Zn, such that the relative orientation of the two ligands is indicated with the ligand sites ordered as  $O_{Pro} > O_{Pro-H} > N_{Pro} > N_{Pro-H}$ . In addition, the nitrogen of the Pro ligand is a stereocenter connected to Zn > C2 > C5 > H.

Theoretical Results: CdCl<sup>+</sup>(Pro) Relative Energies and Structures. Relative single point energies at 0 K and Gibbs energies at 298 K for isomers and conformers of CdCl<sup>+</sup>(Pro) are given in Table 1. Figure 1 shows several of these. At 0 K, all levels of theory predict the [CO<sub>2</sub><sup>-</sup>]cc,C4-endo conformer to be the lowest in energy, whereas at 298 K, the similar [CO<sub>2</sub><sup>-</sup>]cc,C4-exo is the B3LYP global minimum (GM). In both species, a zwitterionic form of proline in which the proton on the carboxylic acid group has migrated to the nitrogen is bound to cadmium via both oxygens of the anionic carboxylate group. These two species differ only in the pucker of the five-membered ring and lie within 3 kJ/mol of one another at all levels of theory.

**Table 1.** Relative energies at 0 K (298 K Gibbs energies) in kJ/mol of CdCl<sup>+</sup>(Pro) complexes<sup>a</sup>

structure	B3LYP	B3P86	MP2(full)
[CO <sub>2</sub> <sup>-</sup> ]cc,C4-endo	0.0 (0.4)	0.0 (0.0)	0.0 (0.0)
[CO <sub>2</sub> <sup>-</sup> ]cc,C4-exo	0.6 (0.0)	1.5 (0.5)	2.5 (1.5)
[N,CO]tt,C4-exo	12.7 (14.4)	10.2 (11.5)	6.2 (7.5)
[N,CO]tt,C4-endo	15.8 (16.4)	12.9 (13.0)	8.7 (8.8)
[N,CO]tc,C4-exo	37.5 (38.5)	34.3 (34.9)	32.0 (32.6)
[N,CO]tc,C4-endo	39.9 (41.4)	36.4 (37.6)	33.5 (34.6)
[N,OH]ct,C5-endo	57.4 (57.5)	57.5 (56.6)	43.0 (43.1)
[N,OH]ct,C5-exo	62.1 (62.0)	61.6 (61.1)	47.6 (47.1)
[COOH]tc,C5-endo	106.3 (103.9)	109.4 (106.0)	118.7 (116.4)
[COOH]tc,C3-exo	109.2 (106.3)	112.0 (108.6)	123.4 (120.1)

<sup>&</sup>lt;sup>a</sup> Relative single point energies calculated at the level of theory indicated using a def2-TZVPP basis set and SDD ECP for Cd using geometries and zero-point and thermal corrections calculated at the B3LYP/def2-TZVP level.

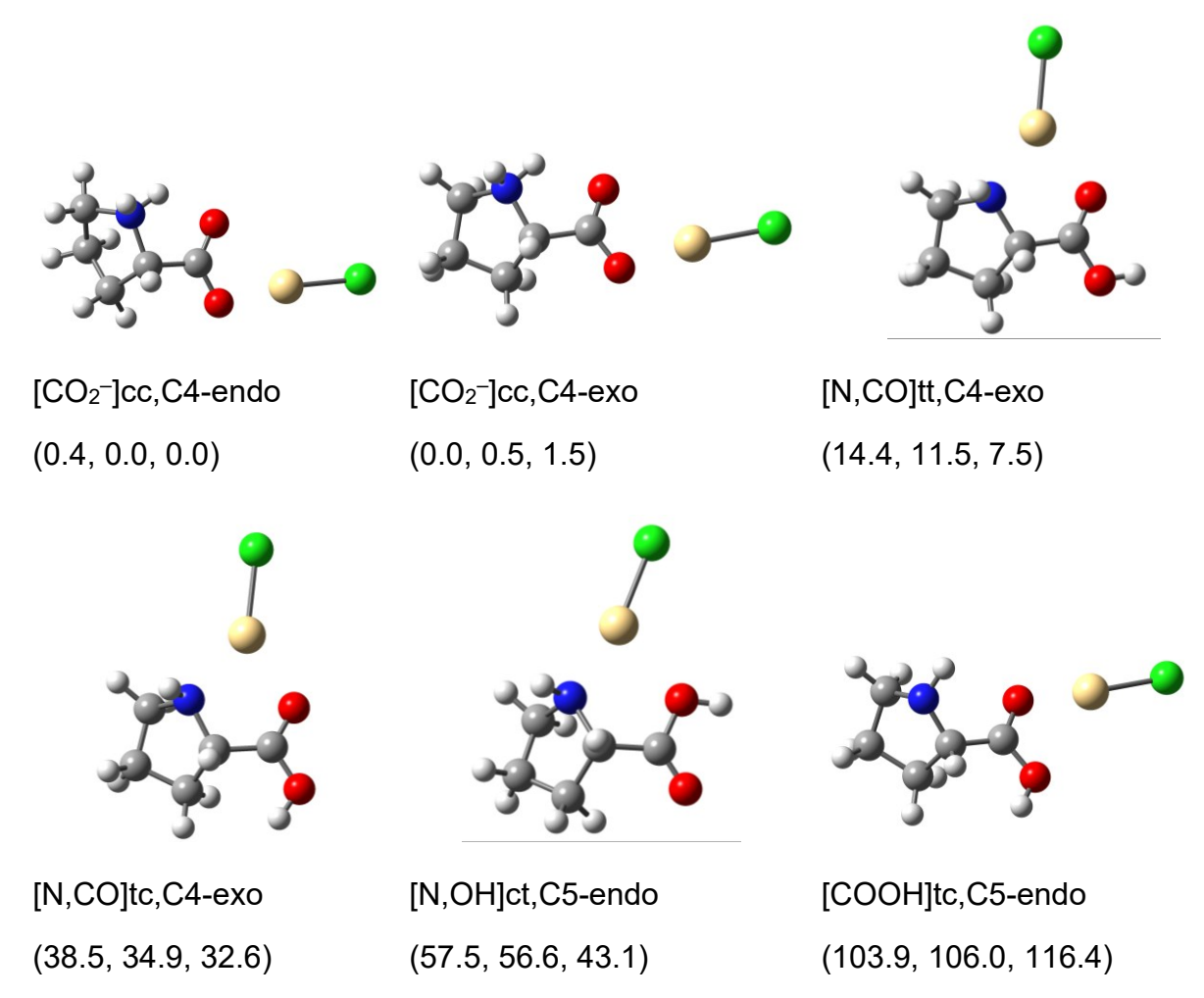


**Figure 1.** Structures of low-energy CdCl<sup>+</sup>(Pro) conformers calculated at the B3LYP/def2-TZVP level of theory. Relative Gibbs energies (298 K) in kJ/mol are given at the B3LYP, B3P86, and MP2(full) levels, respectively. Cadmium – yellow; chlorine – green, carbon – grey; nitrogen – blue; oxygen – red; hydrogen – white.

We also checked the stability of the related [COOH]cc species (both exo and endo forms) in which the metal again binds to both oxygens but now the proton is retained on the carboxylic acid. No stable structure associated with either the C4-endo or C4-exo ring pucker could be located and the potential energy surfaces show that these complexes collapse to the zwitterionic  $[CO_2^-]$  form.

Isomers where cadmium binds to the amine nitrogen and carbonyl oxygen of canonical proline, [N,CO]tt, lie 6 – 16 kJ/mol higher in energy. Again a C4-endo conformer lies 1 – 3 kJ/mol above the lower-energy C4-exo conformer. If the hydrogen on the carboxylic acid group rotates so that it no longer forms a hydrogen bond with the carbonyl oxygen, forming [N,CO]tc structures, the energy rises another 23 – 26 kJ/mol. Likewise, if the hydroxyl oxygen rather than the carbonyl oxygen binds to cadmium, [N,OH]ct, the energy increases by 37 – 49 kJ/mol compared to the [N,CO]tt conformers. Finally, if cadmium binds to the carbonyl oxygen leaning towards the hydroxyl oxygen, but the OH group is rotated so that it cannot form a hydrogen bond interact-with the nitrogen, the [COOH]tc conformers are formed and lie over 100 kJ/mol above the GM at all levels of theory.

Table 2 gives key geometric parameters of the low-energy binding motifs observed for the  $CdCl^+(Pro)$  isomers and conformers. For the  $[CO_2^-]$  structures, cadmium binds tightly to one of the carboxylate oxygens,  $r(Cd-O) \sim 2.1$  Å, but relatively weakly to the second with r(Cd-O) over 2.7 Å. In the high-energy [COOH] structures, which are no longer zwitterionic, the cadmium bond to the carbonyl has a similar length, but the interaction with the other oxygen (now an OH) is longer by 0.3 Å, and therefore much weaker. Bond lengths to the carbonyl oxygens increase to 2.2 -2.3 Å for [N,CO] coordination and cadmium bonds to the hydroxy oxygen in [N,OH] structures are even longer, near 2.45 Å. Interactions with the nitrogens are more uniform with Cd-N bond lengths varying between  $\sim 2.2$  Å for [N,OH] to 2.24 - 2.30 Å for the various [N,CO] species.

**Table 2**. Bond distances (Å) and bond angles (deg) for CdCl<sup>+</sup>(Pro) structures<sup>a</sup>

structure	r(Cd-X)	r(Cd-O)	∠XCdO
[CO <sub>2</sub> <sup>-</sup> ]cc,C4-endo	2.756 <sup>b</sup>	2.111	52.5
[CO <sub>2</sub> <sup>-</sup> ]cc,C4-exo	2.740 <sup>b</sup>	2.114	52.8
[N,CO]tt,C4-exo	2.286	2.304	74.8
[N,CO]tt,C4-endo	2.306	2.284	74.9
[N,CO]tc, C4-exo	2.318	2.263	74.3
[N,CO]tc,C4-endo	2.343	2.241	74.5
[N,OH]ct,C5-endo	2.207	2.445 °	72.4
[N,OH]ct,C5-exo	2.216	2.460 °	72.4
[COOH]tc,C5-endo	3.076 <sup>b</sup>	2.104	45.2
[COOH]tc,C3-exo	3.087 <sup>b</sup>	2.106	44.9

 $<sup>^</sup>a$  Values calculated at the B3LYP/def2-TZVP level of theory. Except as noted, O = carbonyl oxygen and X = amino nitrogen.  $^b$  X = second oxygen in carboxylate or carboxylic acid group.  $^c$  O = hydroxyl oxygen.

Comparison of Experimental and Theoretical IR Spectra: CdCl+(Pro). The main spectral features of the CdCl<sup>+</sup>(Pro) spectrum, Figure 2, are observed at 843, 997, 1170, 1245 (shoulder), 1323, 1420, 1586 (shoulder), and 1610 cm<sup>-1</sup>. The experimental IRMPD action spectrum of CdCl<sup>+</sup>(Pro) is predicted well by the two lowest-energy conformers, [CO<sub>2</sub><sup>-</sup>]cc,C4-endo and [CO<sub>2</sub><sup>-</sup>]cc,C4-exo, which have similar spectra. The major bands predicted for the endo/exo conformers are located at 1635/1632 (CO stretch, NH<sub>2</sub> scissors), 1599/1602 (NH<sub>2</sub> scissors), 1467,1464/1464,1459 (CH<sub>2</sub> scissors), 1401/1402 (C-C2 stretch, CC2H bend), 1373/1339 (CNH bend), 1334/1333 (CCH bends), 1315/1306,1279,1258 (HCN bend and CH<sub>2</sub> wags), 1226/- (HCN bend and NH<sub>2</sub> wag), 1162/1162 (HNC bend, NH<sub>2</sub> and CH<sub>2</sub> twist), 987/994 (ring distortion), 837/835 (ring breathing), and 662/679 cm<sup>-1</sup> (ring distortion). Arguably, the C4-endo spectrum reproduces the experimental spectrum slightly better than that for the C4-exo structure because it more closely matches the relative intensities of the peaks observed at 1323 and 1420 cm<sup>-1</sup> and it captures the shoulder near 1240 cm<sup>-1</sup> and the peak at 843 cm<sup>-1</sup> better. However, especially given its low energy, it seems likely that contributions from the C4-exo structure might also be present. Indeed, Maxwell-Boltzmann distributions at 298 K calculated using the theoretical Gibbs energies indicate populations of 46-62 % for  $[CO_2^-]C4$ -endo and 34-54% for  $[CO_2^-]cc$ , C4-exo. The next lowest energy structure, [N,CO]tt,C4-exo, is calculated to have a population less than 3%. Figure 2 shows that this spectrum is clearly inconsistent with the experimental spectrum, although a small contribution could help explain the broadness of the peak observed at 1610 cm<sup>-1</sup>. Likewise, calculated spectra for the [N,CO]tc and [N,OH]ct structures do not match experiment, Figure 2.

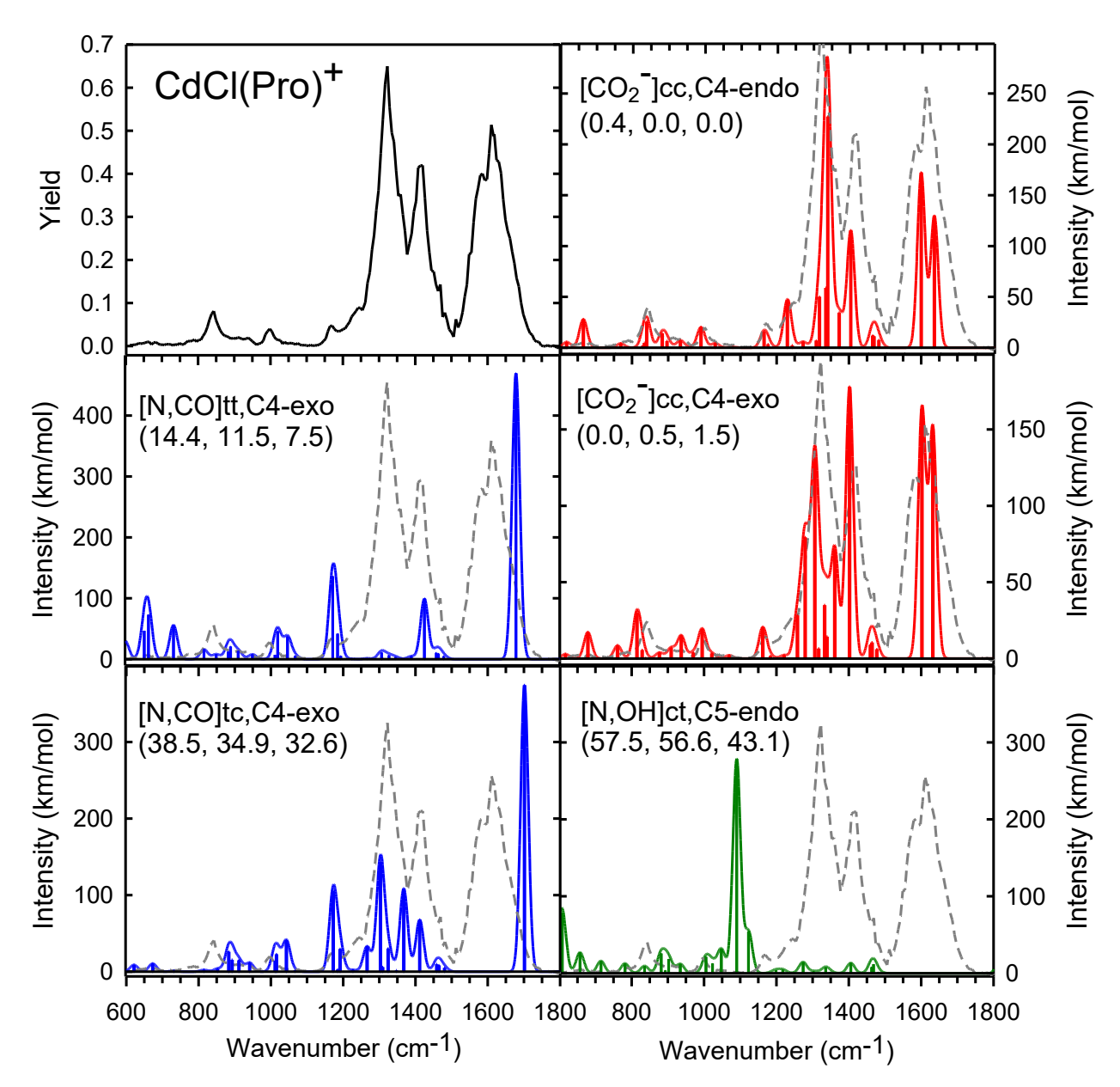


**Figure 2.** Comparison of the CdCl<sup>+</sup>(Pro) experimental IRMPD action spectrum (black, grey) with IR spectra (colored) calculated at the B3LYP/def2-TZVP level of theory for low-lying conformers. Relative 298 K Gibbs energies (kJ/mol) are given at the B3LYP, B3P86, and MP2(full) levels, respectively.

Theoretical Results: Zn<sup>+</sup>(Pro-H)(Pro) Relative Energies and Structures. As noted above, Gholami and Fridgen had performed an extensive exploration of possible structures for these complexes, including explicit consideration of the ring pucker and various [N,CO<sup>-</sup>][N,CO], [N,CO<sup>-</sup>][CO<sub>2</sub><sup>-</sup>], [CO<sub>2</sub><sup>-</sup>][N,CO], [CO<sub>2</sub><sup>-</sup>][CO<sub>2</sub><sup>-</sup>], and [N<sup>-</sup>,CO][N,CO] structures as well as ZnH<sup>+</sup>(Pro-H)(Pro-H) complexes. Their work showed that the complex preferred the [N,CO<sup>-</sup>][N,CO] complexation by 27.2 kJ/mol at the B3LYP level and 16.7 kJ/mol at the MP2 level. (Oddly, the structures shown by Gholami and Fridgen all have prolines with the D enantiomer making comparison with the L-enantiomers more difficult, but because both ligands are altered, the relative energies remain the same and the structures shown are mirror images compared with those shown here.)

Because of these comprehensive results, we only examined the [N,CO-][N,CO] coordination motif and located a number of these conformers with different relative orientations of the ligands and different ring puckers. Our results for the relative single point energies at 0 K and Gibbs energies at 298 K for isomers and conformers of Zn<sup>+</sup>(Pro-H)(Pro) are given in Table 3. Four structures (all R,S) that differ only in the ring puckers lie within 3 kJ/mol of one another at all levels of theory. The lowest of these is shown in Figure 3 and was not located by Gholami and Fridgen, who did find two of the variants, which they called N1 and N3, Table 3. Later, Jami-Alahmadi and Fridgen revisited these structures (using the correct L stereochemistry) and did locate the structure shown in Figure 3 as their global minimum, called NO-NO-CS-X-X-1.<sup>19</sup> They found four of the R,S and S,S structures located here (but did not systematically vary the relative orientation of the two ligands to obtain all eight structures), which they named NO-NO-CS-X(E)-X(E) where X and E stand for exo and endo ring puckers, respectively. Their relative 298 K Gibbs energies calculated at the B3LYP/6-311++G(3d,3p)//B3LYP/6-31+G(d,p) level for these four structures are also included in Table 3. In our work, switching the relative orientation of the two ligands from R to S (giving S,S geometries) increases the energies by 3 – 13 kJ/mol, in agreement with the findings of Fridgen and co-workers for their N2 and N4 conformers and their E-X-3 and E-E-4 conformers, Table 3. If the orientation of the proline ligand is switched from S to R (giving

the R,R structure), the energies increase by about 30 kJ/mol. For the R,R cases, not all variations of the ring pucker were explored, but they are clearly going to be similar in energy to those that were found.

**Table 3.** Relative energies at 0 K (298 K Gibbs energies) in kJ/mol of Zn<sup>+</sup>(Pro-H)(Pro) complexes<sup>a</sup>

[N,CO <sup>-</sup> ][N,CO] structure	B3LYP	B3P86	MP2(full)	Literature <sup>b</sup>
R,S_C4-exo, C4-exo	0.0(0.0)	0.0 (0.5)	2.7 (3.0)	X-X-1 (0.0) <sup>b</sup>
R,S_C4-exo, C4-endo	0.8 (0.1)	0.2 (0.0)	0.4 (0.0)	
R,S_C4-endo, C4-exo	1.6 (2.2)	1.0 (2.1)	2.1 (3.0)	N3 (2.1)/(7.5) <sup>c</sup>
				$X-E-2(0.4)^b$
R,S_C4-endo, C4-endo	2.4 (2.4)	1.3 (1.8)	0.0 (0.3)	N1 (0.0)/(0.0) °
S,S_C4-exo, C4-exo	4.9 (3.3)	5.0 (3.9)	10.6 (9.2)	
S,S_C4-endo, C4-exo	6.7 (6.0)	6.5 (6.3)	10.4 (10.0)	N2 (2.3)/(1.6) °
S,S_C4-exo, C4-endo	8.4 (6.3)	8.2 (6.6)	13.3 (12.1)	E-X-3 (7.5) <sup>b</sup>
S,S_C4-endo, C4-endo	10.4 (9.0)	9.9 (9.0)	12.9 (11.1)	N4 (6.9)/(11.3) <sup>c</sup>
				E-E-4 (10.2) <sup>b</sup>
R,R_C4-exo, N	34.3 (32.4)	34.6 (33.3)	39.8 (38.2)	

<sup>&</sup>lt;sup>a</sup> Relative single point energies calculated at the level of theory indicated using a 6-311+G(2d,2p) basis set using geometries and zero-point and thermal corrections calculated at the B3LYP/6-311+G(d,p) level. <sup>b</sup> 298 K Gibbs energies calculated at the B3LYP/6-311++G(3d,3p)//B3LYP/6-31+G(d,p) level from ref. <sup>19</sup>. <sup>c</sup> 298 K Gibbs energies calculated at the B3LYP/6-31+G(d,p) and MP2(full)/6-311++G(2d,2p)//B3LYP/6-31+G(d,p) levels from ref. <sup>18</sup>.

Table 4 provides selected structural parameters for the [N,CO][N,CO] complexes of Zn<sup>+</sup>(Pro-H)(Pro). It can be seen that the shortest zinc-ligand bonds are those to the deprotonated oxygen, ~1.9 Å. The Zn-O bonds to the intact proline ligand are all about 2.1 Å and the bonds to the nitrogens are ~2.045 Å for Pro-H and ~2.1 Å for Pro. The uniformity of these interactions is consistent with the only differences being ring puckers and relative orientations of identical ligands.

**Table 4**. Bond distances (Å) and bond angles (deg) for Zn<sup>+</sup>(Pro-H)(Pro) structures<sup>a</sup>

	Pro-H			Pro		
[N,CO <sup>-</sup> ][N,CO] Structure	r(Zn-N)	r(Zn-O)	∠NZnO	r(Zn-N)	r(Zn-O)	∠NZnO
R,S_C4-exo,C4-exo	2.044	1.898	89.9	2.097	2.097	81.9
R,S_C4-exo,C4-endo	2.046	1.897	89.9	2.105	2.088	81.8
R,S_C4-endo,C4-exo	2.045	1.896	89.7	2.096	2.098	81.9
R,S_C4-endo,C4-endo	2.045	1.896	89.7	2.096	2.098	81.9
S,S_C4-exo,C4-exo	2.046	1.895	89.8	2.095	2.095	81.3
S,S_C4-endo,C4-exo	2.047	1.894	89.6	2.095	2.103	81.3
S,S_C4-exo,C4-endo	2.046	1.896	89.7	2.103	2.090	81.6
S,S_C4-endo,C4-endo	2.048	1.895	89.7	2.106	2.089	81.6
R,R_C <sub>4</sub> -exo,N	2.041	1.890	90.4	2.077	2.185	78.1

<sup>&</sup>lt;sup>a</sup> Values calculated at the B3LYP/6-311+G(d,p) level of theory. O = carbonyl oxygen and N = amino nitrogen.

Comparison of Experimental and Theoretical IR Spectra: Zn<sup>+</sup>(Pro-H)(Pro). The spectrum of this complex is shown in Figure 3 and exhibits six sharp bands located at 1756, 1687, 1446, 1231, 1171, and 1042 cm<sup>-1</sup>, with a minor band at 839 cm<sup>-1</sup>. As discussed above, there are a multitude of low-energy structures that vary in the pucker of the proline ring and relative placement of the two ligands having [N,CO<sup>-</sup>][N,CO] coordination. Figure 3 shows that these all have similar spectra that closely resemble one another and the experimental spectrum. Figure S1 in the Supporting Information shows that the other variants also have very similar spectra. The 298 K global minimum at the B3LYP level of theory is R,S[N,CO<sup>-</sup>][N,CO]C4-exo,C4-exo, which has its most intense bands predicted at 1737 (uncoordinated CO stretch on Pro-H), 1674 (coordinated CO stretch on Pro), 1426 (COH bend, CC2 stretch, CC2H bend, NH wag on Pro), 1239 (CC2H bend and CH bends on Pro-H), 1175 (COH bend and CH<sub>2</sub> twists on Pro), and 1044 cm<sup>-1</sup> (NH wag and CH<sub>2</sub> twists on Pro-H). A multitude of minor bands predicted below 1000 cm<sup>-1</sup> are not obvious experimentally. Overall, the calculated structures provide a good match to experiment, but the many alternative [N,CO<sup>-</sup>][N,CO] structures cannot be distinguished on the basis of the comparison to experiment. A calculation of the distribution of these structures using the 298 K Gibbs energies indicates that the R,S configurations have 85 - 98% of the population with S,S configurations accounting for the remainder. Of the R,S conformers, the most highly populated one depends on the level of theory but is between 30 and 39%.

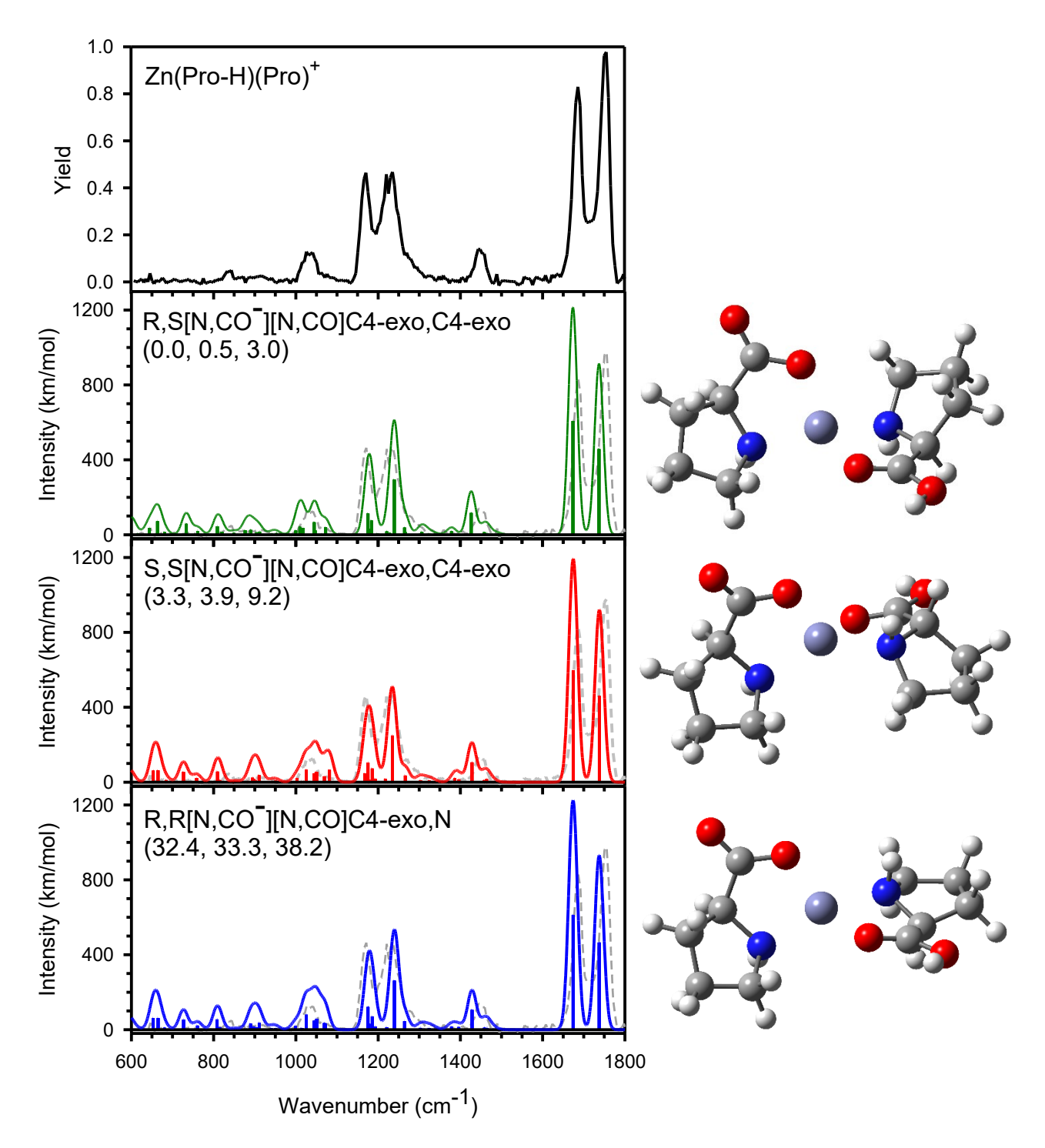


**Figure 3.** Comparison of the Zn<sup>+</sup>(Pro-H)(Pro) experimental IRMPD action spectrum (black, grey) with IR spectra (colored) calculated at the B3LYP/6-311+G(d,p) level of theory for low-lying conformers. Relative 298 K Gibbs energies (kJ/mol) are given at the B3LYP, B3P86, and MP2(full) levels, respectively.

Gholami and Fridgen also examined the IRMPD spectrum of Zn<sup>+</sup>(Pro-H)(Pro) in the hydrogen stretching region observing a band near 3570 cm<sup>-1</sup>,<sup>18</sup> and later, Jami-Alahmadi and Fridgen observed bands at about 3540, 3350, 3000, and 2930 cm<sup>-1</sup>.<sup>19</sup> Their calculated spectra for their [N,CO<sup>-</sup>][N,CO] structures matched these observations well. Our calculated spectrum for the R,S[N,CO<sup>-</sup>][N,CO]C4-exo,C4-exo structure has predicted bands (after scaling by 0.955, the scaling factor used by Fridgen and co-workers and elsewhere in the hydrogen stretching region for protonated polyprolines<sup>37</sup>) of 3548 (OH stretch), 3361 and 3349 (NH stretch of Pro and Pro-H, respectively), and two broad bands between 2950 – 3000 and 2900 – 2950 cm<sup>-1</sup> (various CH stretches) of both proline ligands. Our other [N,CO<sup>-</sup>][N,CO] structures show similar bands that also reproduce the observations of Fridgen and co-workers in this region well.

Theoretical Results: (Zn+Pro-H)+ Relative Energies and Structures. As found by Gholami and Fridgen, 17 the relative energies of ZnH+(Pro-2H) structures are considerably lower in energy than those for Zn<sup>+</sup>(Pro-H). The global minimum (GM) structure, ZnH<sup>+</sup>(Pro-2H) [N,CO]-N,C5, binds the zinc to the nitrogen and the carbonyl oxygen, where dehydrogenation has occurred across the N-C5 bond, Figure 4. This structure matches the GM that was found by Gholami and Fridgen, which they called Pro-Hi, Table 5. About 10 kJ/mol higher in energy at all levels of theory is [N,CO]-N,C2 (Pro-Hii), where dehydrogenation has now occurred across the N-C2 bond. Gholami and Fridgen also located Pro-HC, called [CO]-O,C5 here, in which the zinc binds to a carboxylate oxygen (and leans towards the other oxygen, which has a hydrogen bond with HN) and the C5 position on the ring has lost a hydrogen. In the next highest energy structure, [CO<sub>N</sub>]-O,C5, located 2 – 6 kJ/mol above [CO]-O,C5, the zinc has migrated to the carboxylate oxygen that is hydrogen bonded to HN. We also located an additional seven structures of ZnH<sup>+</sup>(Pro-2H), Table 5, which all lie at least 28 kJ/mol higher than the GM. These include additional [N,CO] and [CO] coordinations, as well as [N,OH] and [CO]-C3,C4,ZW, in which the proline ring has dehydrogenated across the C3-C4 bond and the carboxylic acid proton has migrated to the nitrogen, forming a zwitterionic (ZW) ligand.

We also located several (Pro-H)<sup>+</sup>Zn structures that can be thought of as a dehydrogenated proline (either across the N-C5 or N-C2 bond), the nitrogen is then protonated, and the *neutral* zinc atom hydrogen binds to the NH<sup>+</sup> (as indicated by Zn[NH]). The energies of these complexes vary considerably with the level of theory (see Table 5) and range from 54 to 100 kJ/mol above the GM. Gholami and Fridgen also located such complexes, which they called Pro-Di and Pro-Dii, but did not discuss them in the main body of their paper. Notably, their Di structure differs somewhat from our (Pro-H<sub>C5</sub>)<sup>+</sup>Zn[HN] in that their structure shows the Zn hydrogen bound to HC5 instead of to HN. Our attempts to reproduce this structure collapsed to the one indicated.

Finally, we also explored the more generic structures in which the zinc dication binds to a deprotonated proline, Zn<sup>+</sup>(Pro-H). As for other amino acids previously explored, stable geometries in which the zinc binds to [N,CO<sup>-</sup>], [N<sup>-</sup>,CO], and [N<sup>-</sup>,OH] were located each with two different puckers of the proline ring, Table 5 and Figure 4. A [CO<sub>2</sub><sup>-</sup>]C3-exo structure has only one ring pucker because of strong interactions with the carboxylate group. Several of these were also located by Gholami and Fridgen and called Pro-A, B, and C. As they did not explicitly consider the ring pucker, the lowest energy structure of this type, Pro-B, equivalent here to [N,CO<sup>-</sup>]C4-endo, was not the lowest energy structure we found, which was [N,CO<sup>-</sup>]C4-exo, 1 – 3 kJ/mol lower. Further, Gholami and Fridgen also located two tridentate geometries, which they called Pro-Ei and Pro-Eii, that were not included in the main text but shown in their Supporting Information. In these structures, named [N,CO,C4<sup>-</sup>] (Figure 4) and [N,CO,C3<sup>-</sup>] here, respectively, deprotonation has occurred on the ring at either C4 or C3, which then forms a strong complexation site for zinc along with the nitrogen and carbonyl oxygen. In agreement with the calculations of Gholami and Fridgen, we find that the [N,CO,C4<sup>-</sup>] structure lies below the bidentate [N,CO<sup>-</sup>]C4-endo by 8 – 16 kJ/mol.

**Table 5.** Relative energies at 0 K (298 K Gibbs energies) in kJ/mol of (Zn+Pro-H)<sup>+</sup> complexes<sup>a</sup>

structure	B3LYP	B3P86	MP2(full)	Literature <sup>b</sup>
ZnH <sup>+</sup> (Pro-2H)				
[N,CO]-N,C5	0.0 (0.0)	0.0 (0.0)	0.0 (0.0)	Pro-Hi (0.0)/(0.0)
[N,CO]-N,C2	9.9 (8.5)	11.0 (9.5)	11.1 (9.7)	Pro-Hii (10.2)/(11.6)
[CO]-O,C5	17.3 (12.6)	23.5 (18.7)	27.7 (23.0)	Pro-HC (12.9)/(23.0)
$[CO_N]$ -O,C5	22.3 (16.0)	27.5 (21.3)	33.3 (27.1)	
[N,OH]-N,C5	33.9 (32.8)	36.5 (35.4)	29.7 (28.6)	
[N,OH]-N,C2	37.0 (35.2)	40.5 (38.7)	34.0 (32.2)	
[CO]-C3,C4,ZW	42.8 (39.0)	48.4 (44.5)	49.2 (45.3)	
[N,CO]-C3,C4	47.0 (46.2)	46.4 (45.6)	46.5 (45.7)	
[CO]-N,C5	62.4 (59.4)	66.6 (63.6)	75.0 (72.0)	
[CO]-N,C2	67.1 (62.6)	73.2 (68.7)	83.7 (79.1)	
[N,OH]-C3,C4	95.5 (93.8)	97.7 (96.0)	88.5 (86.9)	
(Pro-H) <sup>+</sup> Zn				
$(Pro-H_{C5})^{+}Zn[HN]$	67.1 (54.2)	88.5 (75.6)	94.2 (81.3)	Pro-Di (62.2)/(96.9)
(Pro-H <sub>C2</sub> ) <sup>+</sup> Zn[HN]	70.9 (56.9)	93.7 (78.7)	100.0 (86.0)	Pro-Dii (59.5)/(96.2)
Zn <sup>+</sup> (Pro-H)				
[N,CO,C4 <sup>-</sup> ]	133.1 (136.5) °	115.8 (119.2)°	106.1 (109.5)°	Pro-Ei (102.6)/(109.0) °
	0.0 (0.0)	0.0 (0.0)	0.0 (0.0)	(0.0)/(0.0)
[N,CO <sup>-</sup> ]C4-exo	8.0 (5.3)	15.8 (13.1)	12.9 (10.2)	
[N,CO <sup>-</sup> ]C4-endo	11.0 (8.4)	18.2 (15.6)	14.2 (11.6)	Pro-B (40.0)/(8.8)
[N,CO,C3 <sup>-</sup> ]	22.4 (20.6)	24.1 (22.3)	26.6 (24.8)	Pro-Eii (28.4)/(25.5)
[N <sup>-</sup> ,CO]tt,C5-exo	26.2 (23.7)	34.3 (31.8)	43.1 (40.6)	
[N <sup>-</sup> ,CO]tt,C3-endo	29.7 (24.8)	36.7 (32.9)	45.9 (42.1)	Pro-A (60.5)/(39.4)
$[\mathrm{CO_2}^-]\mathrm{C3}\text{-exo}$	39.0 (32.1)	57.4 (50.5)	121.8 (114.9)	Pro-C (64.5)/(105.4)

[N-,CO]tc,C4-exo	42.7 (40.2)	49.6 (47.0)	57.6 (55.0)
[N <sup>-</sup> ,CO]tc,C3-endo	45.3 (42.2)	51.8 (48.7)	59.5 (56.3)
[N-,OH]N-endo	90.5 (86.5)	104.2 (100.2)	103.7 (99.7)

<sup>&</sup>lt;sup>a</sup> Relative single-point energies calculated at the level of theory indicated using a 6-311+G(2d,2p) basis set using geometries and zero-point and thermal corrections calculated at the B3LYP/6-31+G(d,p) level. <sup>b</sup> 298 K Gibbs energies calculated at the B3LYP/6-31+G(d,p) and MP2(full)/6-311++G(2d,2p)//B3LYP/6-31+G(d,p) levels from ref. <sup>17</sup>. <sup>c</sup> This is the relative energy with respect to the global minimum of ZnH<sup>+</sup>(Pro-2H).

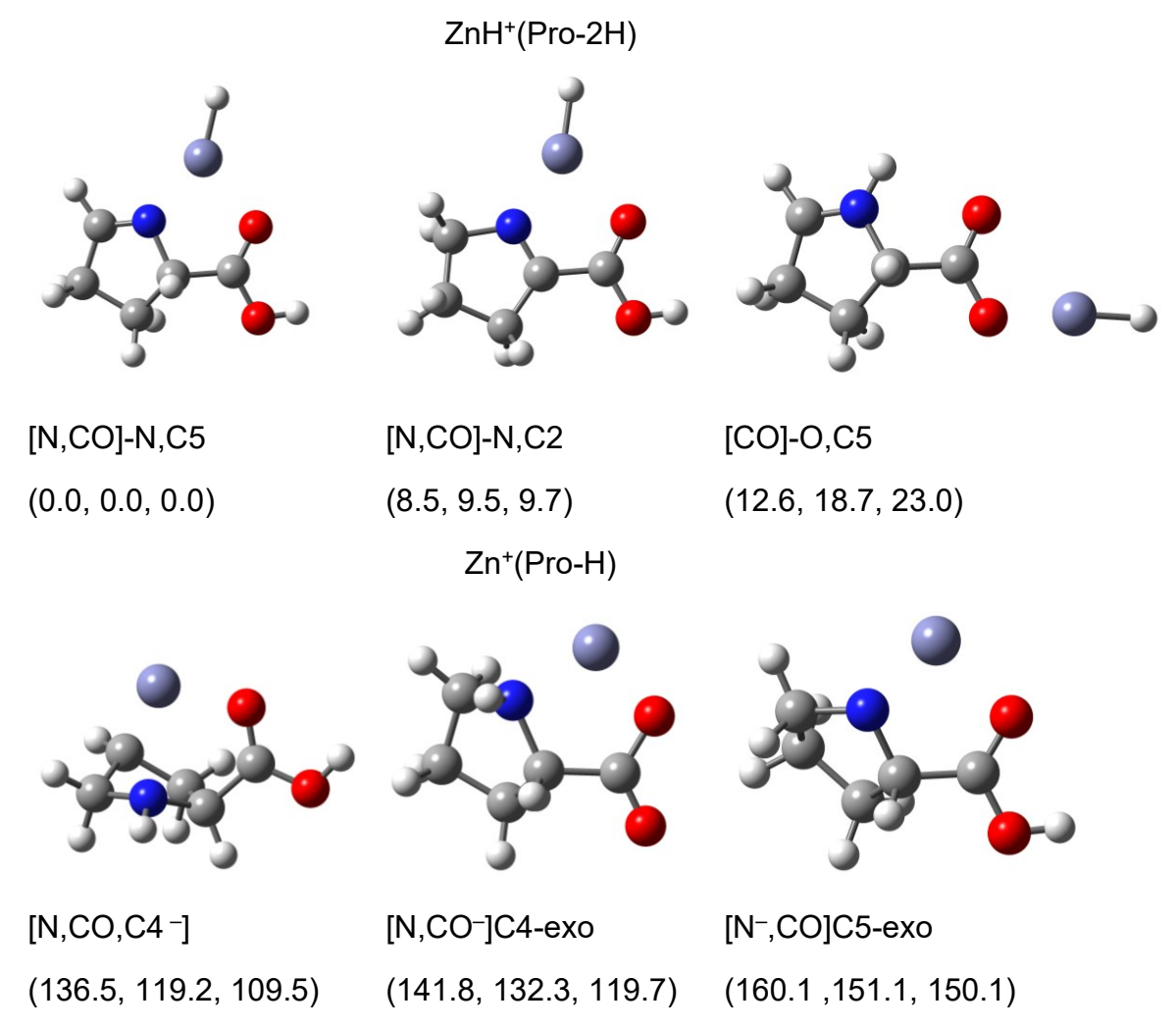


**Figure 4.** Structures of select (Zn+Pro-H)<sup>+</sup> isomers calculated at the B3LYP/6-311+G(d,p) level of theory. Relative Gibbs energies (298 K) are given at the B3LYP, B3P86, and MP2(full) levels, respectively. Zinc – steel blue; carbon – grey; nitrogen – blue; oxygen – red; hydrogen – white.

A description of the key geometric parameters of each major identified binding motif for the (Zn+Pro-H)<sup>+</sup> isomers and conformers is given in Table 6, where our structural analysis provides valuable information regarding the binding affinity and conformational effects in these complexes. For the ZnH<sup>+</sup>(Pro-2H) and Zn<sup>+</sup>(Pro-H) isomers, zinc bond lengths to nitrogen sites are relatively uniform varying between 2.0 and 2.1 Å; however, when the nitrogen is deprotonated as in the [N<sup>-</sup>,CO] structures of Zn<sup>+</sup>(Pro-H), these bond lengths decrease by about 0.1 Å. For the tridentate Zn<sup>+</sup>(Pro-H) [N,CO,CX<sup>-</sup>] structures, the Zn-N bond lengths increase to nearly 2.5 Å because of the favorability of binding to the carbanion site. Zinc bonds to carbonyl oxygens are shortest when these are a carboxylate, about 1.9 Å for ZnH<sup>+</sup>(Pro-2H) and 1.84 Å for Zn<sup>+</sup>(Pro-H). The exception is the Zn<sup>+</sup>(Pro-H) [CO<sub>2</sub><sup>-</sup>]C3-exo structure where the zinc bonds to both oxygens are nearly equal in length and therefore somewhat longer at 2.08 Å. For structures containing the carboxylic acid group, the Zn-O bond lengths increase up to 2.2 Å for the ZnH<sup>+</sup>(Pro-2H) [N,CO]-N,C2 structure and to 2.0 - 2.1 Å for the [N,CO] structures of Zn<sup>+</sup>(Pro-H). Bond lengths between zinc and the hydroxyl oxygen are longer by about 0.1 Å for similar structures, consistent with the weaker binding energies. For all five [CO] structures of ZnH<sup>+</sup>(Pro-2H), there is a weak interaction with the other oxygen of the carboxylate, in [CO]-O,C5 structures, or carboxylic acid, in [CO]-N,CX structures, consistent with the long bond lengths of 2.7 - 2.9 Å and  $\sim 3.2$  Å, respectively.

**Table 6.** Bond distances (Å) and bond angles (deg) for (Zn+Pro-H)<sup>+</sup> structures<sup>a</sup>

structure	r(Zn-X)	r(Zn-O)	r(Zn-C)	∠XZnO	∠XZnC	∠OZnC
ZnH <sup>+</sup> (Pro-2H)						
[N,CO]-N,C5	2.045	2.157		77.7		
[N,CO]-N,C2	2.054	2.202		77.4		
[CO]-O,C5	1.891 <sup>b</sup>	2.905		50.7		
$[CO_N]$ -O,C5	1.918 <sup>b</sup>	2.695		54.9		
[N,OH]-N,C5	1.994	2.269°		75.4		

[N,OH]-N,C2	1.997	2.315°		74.9		
[CO]-C3,C4,ZW	$3.020^{b}$	1.887		93.3		
[N,CO]-C3,C4	2.128	2.071		80.8		
[CO]-N,C5	3.158 <sup>b</sup>	1.906		43.6		
[CO]-N,C2	3.156 <sup>b</sup>	1.910		43.7		
[N,OH]-C3,C4	2.051	2.165°		78.8		
(Pro-H) <sup>+</sup> Zn						
$(Pro-H_{C5})^{+}Zn[HN]$	2.673	4.197		35.8		
$(Pro-H_{C2})^{+}Zn[HN]$	2.737	4.068		36.4		
Zn <sup>+</sup> (Pro-H)						
[N,CO,C4 <sup>-</sup> ]	2.547	2.062	2.029	76.5	58.7	111.5
[N,CO <sup>-</sup> ]C4-exo	1.990	1.844		98.1		
[N,CO <sup>-</sup> ]C4-endo	1.993	1.842		98.1		
[N,CO,C3 <sup>-</sup> ]	2.503	2.141	2.047	77.1	59.2	91.4
[N <sup>-</sup> ,CO]tt,C5-exo	1.898	2.053		90.3		
[N <sup>-</sup> ,CO]tt,C3-endo	1.886	2.047		90.9		
[CO <sub>2</sub> <sup>-</sup> ]C3-exo	$2.078^{b}$	2.082		63.8		
[N <sup>-</sup> ,CO]tc,C4-exo	1.894	2.022		91.1		
[N <sup>-</sup> ,CO]tc,C3-endo	1.882	2.019		91.7		
[N <sup>-</sup> ,OH]N-endo	1.994	2.269 <sup>c</sup>		75.4		

<sup>&</sup>lt;sup>a</sup> Values calculated at the B3LYP/6-311+G(d,p) level of theory. Except as noted, O = carbonyl oxygen of backbone and X = amino nitrogen.  $^bX = \text{second oxygen in carboxylic acid or carboxylate group}$ .  $^cO = \text{hydroxyl oxygen}$ .  $^dX = \text{H on N}$ .

A comparison of the bond lengths in Zn(Pro-H)<sup>+</sup> complexes to CdCl<sup>+</sup>(Pro) structures characterized by a similar binding motif shows that the latter exhibit longer M-O and M-X bonds. This reflects the smaller ionic radius of Zn<sup>2+</sup> (0.60 Å) as compared to that of Cd<sup>2+</sup> (0.78 Å),<sup>38</sup> but is most directly influenced by the tighter binding in the Zn<sup>+</sup>(Pro-H) complexes resulting from the stronger electrostatic interactions between the metal center and deprotonated anion ligand as compared with the intact, neutral amino acid in the CdCl<sup>+</sup> complexes.

Comparison of Experimental and Theoretical IR Spectra: (Zn+Pro-H)<sup>+</sup>. As shown in Figure 5, the main spectral features for the (Zn+Pro-H)<sup>+</sup> complex are observed at 723, 1165, 1435, 1618, and 1680 cm<sup>-1</sup>, with minor peaks at 980 and 1047 cm<sup>-1</sup> and a broad band centered at 1300 cm<sup>-1</sup>. Comparisons to a number of structures for Zn<sup>+</sup>(Pro-H) reveal no species that match the experimental spectrum. In particular, the CO stretches, which lie between 1600 – 1800 cm<sup>-1</sup> clearly do not match the observed spectrum. Of these structures, Gholami and Fridgen concluded that only [N<sup>-</sup>,CO] coordination (which they called Pro-A) had an intense OH stretch band in the region of 3200 – 3800 cm<sup>-1</sup> that matched the single peak observed at 3557 cm<sup>-1</sup> in their experiment. In addition, we note that the [N,CO,C4<sup>-</sup>] and [N,CO,C3<sup>-</sup>] structures both have a band at the right position. Although the [N<sup>-</sup>,CO] structure could not be eliminated spectroscopically at that time, the comparison here clearly shows that this structure cannot be the species observed experimentally. In contrast, the [N,CO,CX<sup>-</sup>] species do reproduce many of the experimental bands but not the most intense band at 1680 cm<sup>-1</sup>.

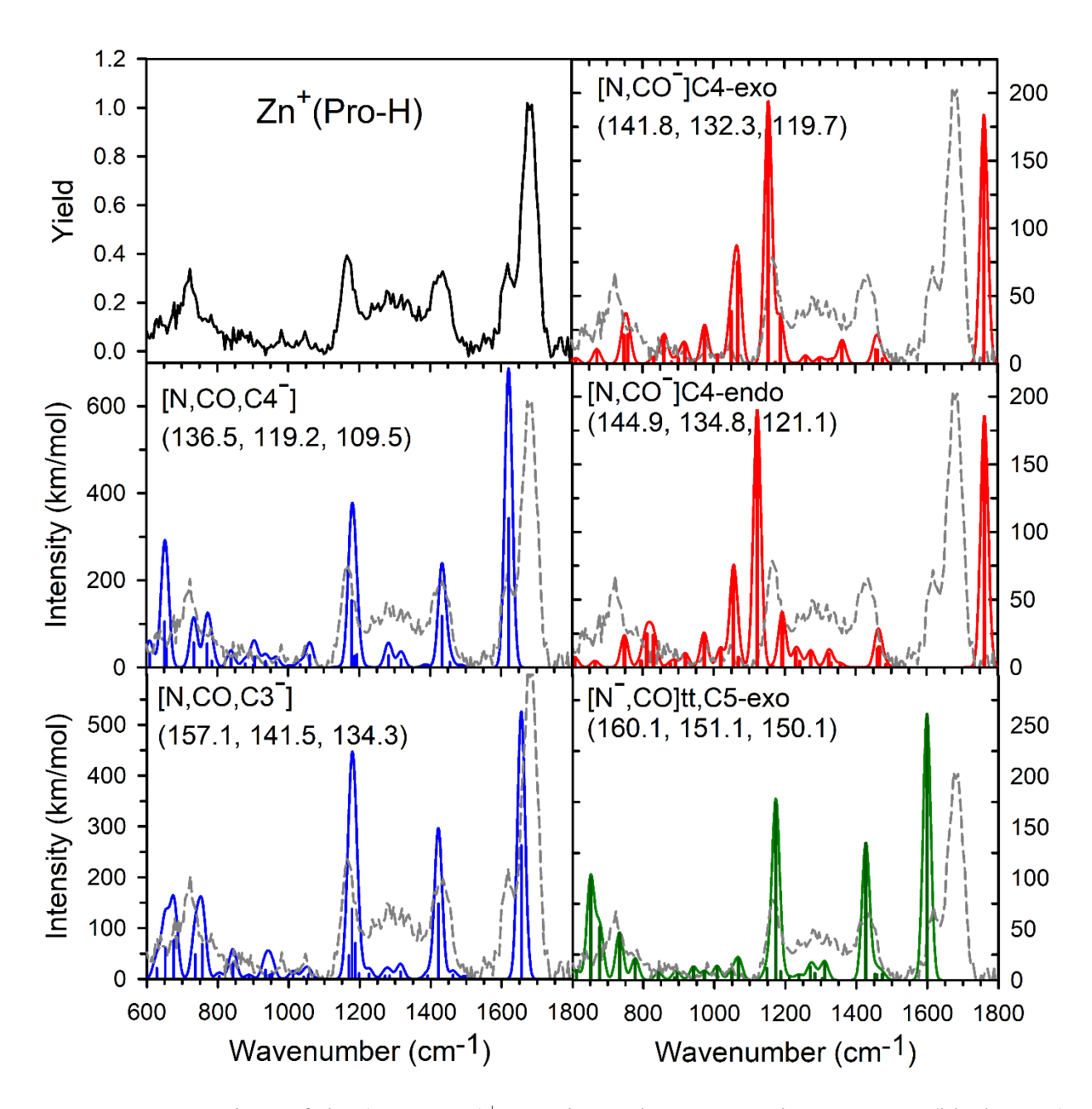


**Figure 5.** Comparison of the (Zn+Pro-H)<sup>+</sup> experimental IRMPD action spectrum (black, grey) with IR spectra (colored) calculated at the B3LYP/6-311+G(d,p) level of theory for low-lying conformers of Zn<sup>+</sup>(Pro-H). 298 K Gibbs energies (kJ/mol) are given at the B3LYP, B3P86, and MP2(full) levels, respectively.

These authors also considered the possibility that one of the hydrogen atoms had migrated to the Zn, leading to a ZnH<sup>+</sup>(Pro-2H) complex. Figure 6 shows a comparison between the three lowest energy structures of this type and the experimental spectrum. It is clear that the two [N,CO] spectra, [N,CO]-N,C5 and [N,CO]-N,C2 (called Pro-Hi and Pro-Hii by Gholami and Fridgen) match the experimental spectrum fairly well. Their spectra ([N,CO]-N,C5/[N,CO]-N,C2) reproduce the main bands at 1672/1697 (CO stretch), 1633/1645 (C5N stretch and NC5H bend/ C2N stretch), 1425,1421/1423,1420 (COH and CC2H bends, C-OH stretch, and CH<sub>2</sub> scissors), 1180/1178 cm<sup>-1</sup> (in-plane COH bend) along with several bands near 1300 cm<sup>-1</sup> (various CH bends and CH<sub>2</sub> wags and twists). Both species also have a series of bands between 600 and 800 cm<sup>-1</sup> (largely out-of-plane COH bend) where experimental intensity also arises. The [N,CO]-N,C5 also has a pair of weak bands at 1033 (C2C3 stretch) and 996 cm<sup>-1</sup> (CC2 stretch) that reproduce these weak experimental bands. (These bands shift to 997 and 969 cm<sup>-1</sup> for [N,CO]-N,C2.) Arguably, the [N,CO]-N,C5 spectrum matches experiment slightly better, but both isomers could contribute in the experiment. Notably, these two structures also have an intense band at 3537/3533 cm<sup>-1</sup> (scaled by 0.955) that matches the band observed by Gholami and Fridgen at 3557 cm<sup>-1</sup>. The spectrum of the third structure shown, [CO]-O,C5, no longer has an OH stretch and furthermore can be seen to miss the peaks observed at 1165 and 1618 cm<sup>-1</sup>, Figure 6. We conclude that the ZnH<sup>+</sup>(Pro-H) [N,CO] species are present, confirming the identification of Fridgen and co-workers on the basis of the OH stretch and calculated energies.

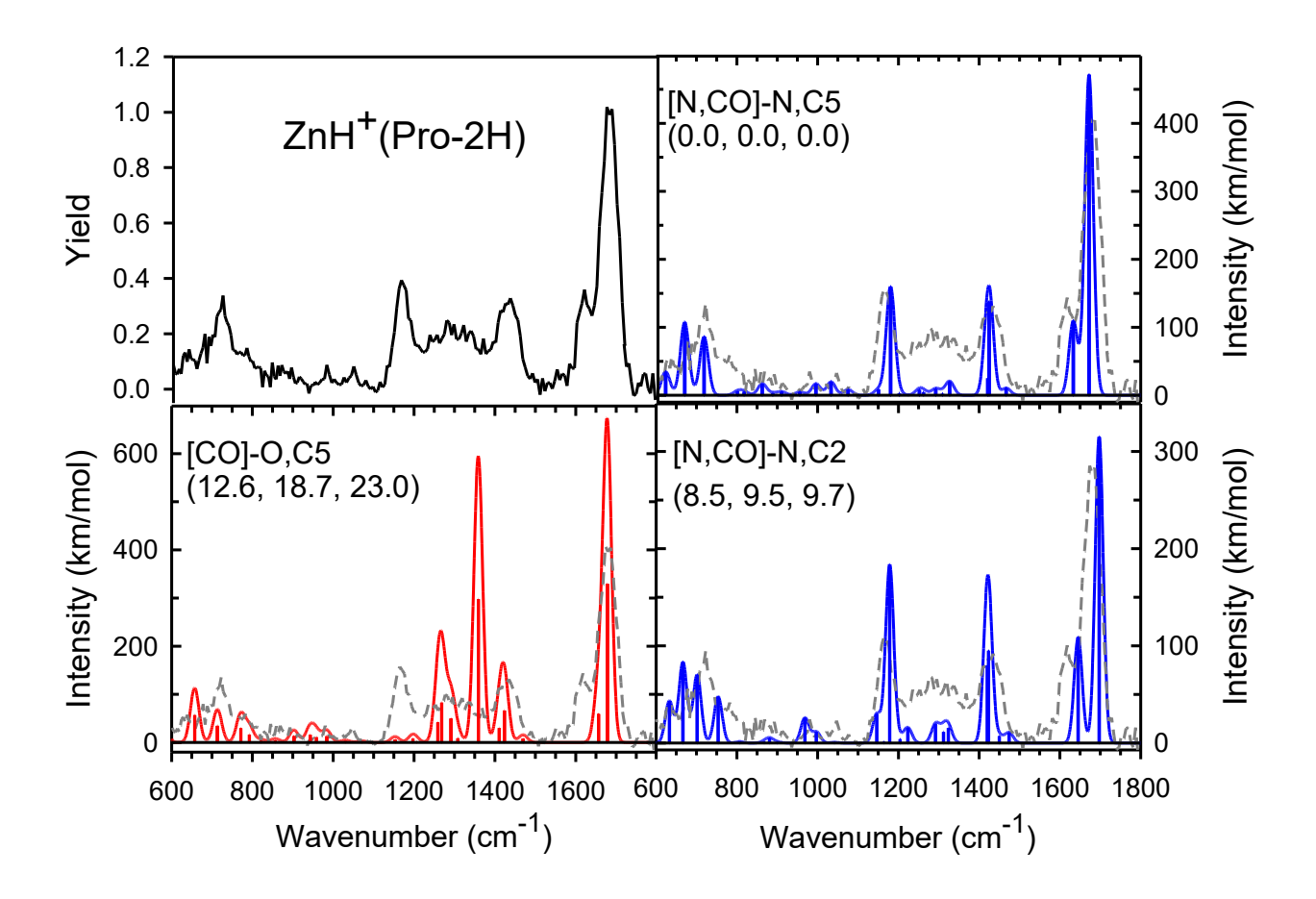


**Figure 6.** Comparison of the (Zn+Pro-H)<sup>+</sup> experimental IRMPD action spectrum (black, grey) with IR spectra (colored) calculated at the B3LYP/6-311+G(d,p) level of theory for low-lying conformers of ZnH<sup>+</sup>(Pro-2H). Relative 298 K Gibbs energies (kJ/mol) are given at the B3LYP, B3P86, and MP2(full) levels, respectively.

Mechanism for Rearrangement. A key finding of Ohanessian and co-workers was that the rearrangement of Zn<sup>+</sup>(Gly-H) to ZnH<sup>+</sup>(Gly-2H) occurred in the gas phase as the solvent was lost, i.e., the solvent molecule facilitated the hydrogen transfer as long as desolvation was energetically more costly. <sup>1-4</sup> To investigate whether the same result holds for the proline analogue, we examined the potential energy profile for desolvation versus rearrangement. The results are tabulated in Table 7 as calculated at the L/6-311+G(2d,2p)//B3LYP/6-311+G(d,p) level where L = B3LYP, B3P86, and MP2(full). Figure 7 shows the B3LYP and MP2 results along with the associated structures of intermediates and transition states. (Only results for the C4-exo ring pucker were explored. Similar energetics are expected for a C4-endo pucker.) It can be seen that the (CH<sub>3</sub>OH)Zn<sup>+</sup>(Pro-H)[N,CO<sup>-</sup>] species requires about 200 kJ/mol to desolvate at 0 K. Alternatively, this complex can transfer a proton from methanol to proline, yielding (CH<sub>3</sub>O)Zn<sup>+</sup>(Pro)[N,OH], and rearrange by rotation of the carboxylic acid to form (CH<sub>3</sub>O)Zn<sup>+</sup>(Pro)[N,CO]. Then, a proton on nitrogen transfers back to the anionic methoxy ligand to yield (CH<sub>3</sub>OH)Zn<sup>+</sup>(Pro-H)[N<sup>-</sup>,CO]. Energetically, the most difficult step is the following transfer of a hydrogen from C5 to Zn, leading to (CH<sub>3</sub>OH)ZnH<sup>+</sup>(Pro-2H)[N,CO]-N,C5. This step requires 152 – 174 kJ/mol but lies 29 – 42 kJ/mol below the initial desolvation step. Desolvation of this latter intermediate requires only 70 – 90 kJ/mol, substantially less than from (CH<sub>3</sub>OH)Zn<sup>+</sup>(Pro-H)[N,CO<sup>-</sup>] because ZnH<sup>+</sup> has a lower charge density than the bare Zn.

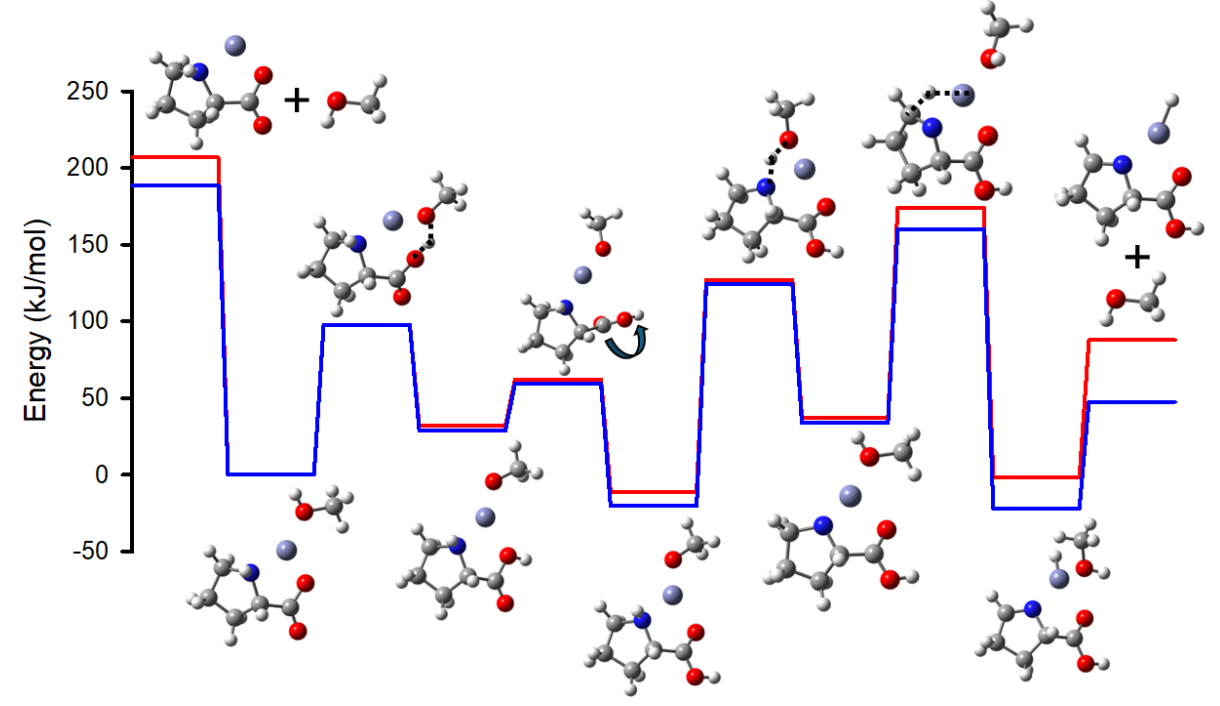


**Figure 7.** Mechanism for rearrangement of the Zn<sup>+</sup>(Pro-H)(CH<sub>3</sub>OH) complex calculated at the B3LYP/6-311+G(d,p) level of theory. Relative energies are determined at the B3LYP/6-311+(2d,2p) (blue lines) and MP2(full)/6-311+(2d,2p) (red lines) including zero-point corrections. Species listed in Table 7 are shown left to right.

**Table 7**. Relative energies at 0 K (298 K Gibbs energies) in kJ/mol of (Zn+Pro-H)(CH<sub>3</sub>OH)<sup>+</sup> complexes. All complexes retain the C4-exo ring pucker.<sup>a</sup>

structure	B3LYP	B3P86	MP2(full)
$Zn^{+}(Pro-H)[N,CO^{-}] + CH_3OH$	188.7 (147.8)	194.5 (153.7)	206.8 (166.0)
$(CH_3OH)Zn^+(Pro-H)[N,CO^-]$	0.0 (0.0)	0.0 (0.0)	0.0 (0.0)
TS	97.6 (103.3)	90.6 (96.3)	97.8 (103.6)
(CH <sub>3</sub> O)Zn <sup>+</sup> (Pro)[N,OH]	28.8 (26.3)	30.9 (28.3)	31.9 (29.4)
TS	59.5 (59.4)	64.0 (63.8)	62.0 (61.9)
(CH <sub>3</sub> O)Zn <sup>+</sup> (Pro)[N,CO]	-20.4 (-19.9)	-2.0 (-1.5)	-11.0 (-10.5)
TS	124.4 (130.2)	113.9 (119.7)	127.1 (132.9)
$(CH_3OH)Zn^+(Pro-H)[N^-,CO]$	33.8 (32.9)	32.6 (31.7)	37.2 (36.3)
TS	160.0 (159.9)	152.1 (151.9)	174.0 (173.8)
(CH <sub>3</sub> OH)ZnH <sup>+</sup> (Pro-2H)[N,CO]-N,C5	-22.0 (-23.3)	-10.6 (-11.9)	-1.7 (-3.1)
$ZnH^{+}(Pro-2H)[N,CO]-N,C5+CH_{3}OH$	47.6 (6.1)	62.9 (21.4)	87.8 (46.2)

<sup>&</sup>lt;sup>a</sup> Relative single-point energies calculated at the level of theory indicated using a 6-311+G(2d,2p) basis set including zero-point and thermal corrections and using B3LYP/6-311+G(d,p) geometries.

We also explored the analogous process for solvation by water instead of methanol at the same levels of theory. This reaction coordinate parallels that for methanol and is shown in Supporting Information Figure S3 with energies in Table S1. Now, dehydration of (H<sub>2</sub>O)Zn<sup>+</sup>(Pro-H)[N,CO<sup>-</sup>] requires 161 – 174 kJ/mol, such that the water ligand is bound less strongly than methanol by 25 – 33 kJ/mol. Here, the rate limiting step, again transfer of H from C5 to Zn, lies at 145 – 166 kJ/mol, 8 – 24 kJ/mol below the initial dehydration step. Dehydration of the (H<sub>2</sub>O)ZnH<sup>+</sup>(Pro-2H)[N,CO]-N,C5 complex requires only 52 – 72 kJ/mol and the overall process is endothermic by 20 – 55 kJ/mol. As for the methanol case, the rearrangement to the zinc hydride complex requires less energy than the initial desolvation step.

It is also interesting to consider the thermodynamics of the rearrangement process. The ZnH<sup>+</sup> bond dissociation energy (BDE) at 0 K has been measured as  $228 \pm 13$  kJ/mol.<sup>39</sup> In good agreement, we calculate here that this BDE is 225 kJ/mol at the B3LYP/6-311+G(2d,2p)//B3LYP/6-311+(G,d,p) level (232 and 192 kJ/mol for B3P86 and MP2(full), respectively). Given that this is substantially smaller than most CH, NH, and OH bonds, the driving force for generating ZnH<sup>+</sup> might seem lacking; however, the appropriate bond to consider is removal of H from the radical (Pro-H). Here, theory indicates that loss of H from C5 in the (Pro-H)-N radical (where the H atom has been lost from nitrogen), the BDE for forming (Pro-2H)-N,C5 is 131 kJ/mol at the same level of theory (142 and 87 kJ/mol at B3P86 and MP2(full), respectively). This CH bond is much weaker than normal because a C5-N  $\pi$  bond is formed as the hydrogen atom is removed.

Finally, we note that any appropriate molecule that solvates Zn<sup>+</sup>(Pro-H) can probably induce this rearrangement during desolvation. Thus, it seems plausible that loss of the Pro ligand from the Zn<sup>+</sup>(Pro-H)(Pro) complex would also lead to ZnH<sup>+</sup>(Pro-2H), although this was not directly confirmed experimentally. Notably, if a ZnH<sup>+</sup>(Pro-2H)(Pro) complex was formed, it could also lose the (Pro-2H) ligand, leading to formation of ZnH<sup>+</sup>(Pro) as the (Zn+Pro+H)<sup>+</sup> species noted above.

Comparison to Akali Cation Complexes of Proline. In previous work, the IRMPD spectra of the five alkali monocations complexed with proline were examined and compared to theoretically predicted spectra. 40-42 In parallel with the present calculations for CdCl<sup>+</sup>(Pro), the lowest energy structure for all five alkali complexes is the [CO<sub>2</sub><sup>-</sup>]cc,C4-endo structure, with C4-exo being low lying. The IRMPD spectra for Li<sup>+</sup>(Pro) and Na<sup>+</sup>(Pro) indicate that these two structures, which have very similar spectra, can explain the observed spectra. In contrast, for K<sup>+</sup>(Pro), Rb<sup>+</sup>(Pro), and Cs<sup>+</sup>(Pro), a shoulder to the blue of the carbonyl stretch peak near 1650 cm<sup>-1</sup> grows in as one moves down the periodic table. This is evidence for [COOH]cc structures, where the carbonyl stretch is near 1750 cm<sup>-1</sup>. In agreement, B3LYP theory predicts that the energy difference between the zwitterionic and charge solvated forms drops from 26.5 kJ/mol for Na<sup>+</sup>(Pro), to 14.5 kJ/mol for K<sup>+</sup>(Pro), to 5.9 kJ/mol for Rb<sup>+</sup>(Pro), to 1.8 kJ/mol for Cs<sup>+</sup>(Pro). For Li<sup>+</sup>(Pro), the charge solvated [COOH]cc forms collapse to the zwitterionic [CO<sub>2</sub><sup>-</sup>]. Thus, the CdCl<sup>+</sup>(Pro) results obtained here parallel the smallest alkali cations, presumably because of the partial doubly charged character on cadmium in the CdCl<sup>+</sup> moiety.

Comparison to Other Amino Acids. As described in the introduction, most other amino acids complex with Zn by deprotonation to form a Zn<sup>+</sup>(Xxx-H) complex having a [N,CO<sup>-</sup>,SC] coordination, although both Cys and Thr will also deprotonate the side chain instead. In contrast, both glycine and proline rearrange to primarily yield a ZnH<sup>+</sup>(Xxx-2H)[N,CO] complex. Ohanessian and co-workers thoroughly investigated this rearrangement process for the glycine case, <sup>1-4</sup> concluding that the deprotonated [N,CO<sup>-</sup>] species is formed in solution but then rearranges as the complex desolvates during the electrospray ionization process. As they showed computationally, this rearrangement requires less energy than desolvation, a conclusion also found here for the proline analogue, Figure 7. Generally, when the amino acid has a functionalized side chain, complexation with the side chain substitutes for the last solvent molecule in this process. Because it is difficult to lose the side chain because of its proximity, desolvation becomes the energetically preferred pathway during the electrospray process and the rearrangement to form the

ZnH<sup>+</sup> species is generally suppressed. Notably, asparagine and aspartic acid have a competing dissociation pathway that involves deamination, leading to (NH<sub>3</sub>)Zn<sup>+</sup>(Xxx-NH<sub>4</sub>) products. <sup>14-15</sup>

## **Conclusions**

IRMPD action spectra for complexes of proline cationized with Zn<sup>2+</sup> and Cd<sup>2+</sup> were measured in the region of 600 - 1850 cm<sup>-1</sup> and were compared to IR spectra calculated at the B3LYP/6-311+G(d,p) and B3LYP/def2-TZVP levels of theory, respectively. For CdCl<sup>+</sup>(Pro), the theoretically determined global minimum, [CO2<sup>-</sup>]C4,endo, has a spectrum that reproduced the experimental spectrum well, although the alternate C4-exo conformer might also contribute. This result parallels findings for alkali metal cations complexed with Pro. For the Zn<sup>+</sup>(Pro-H)(Pro) complex, an [N,CO<sup>-</sup>][N,CO] conformer is consistent with the experimental spectrum, in agreement with the conclusions of Gholami and Fridgen. <sup>18</sup> A variety of different ring puckers and orientations of the two ligands were explored but yield theoretical spectra that vary little, such that several geometries are likely to be experimentally populated. For the (Zn+Pro-H)+ complex, the rearranged ZnH<sup>+</sup>(Pro-2H)[N,CO]-N,C5 species, the global minimum, has a predicted spectrum in good agreement with the observed spectrum, again in good agreement with the conclusions of Gholami and Fridgen on the basis of a single OH stretch band and theory.<sup>17</sup> It is possible that Zn<sup>+</sup>(Pro-H) species deprotonated on the proline ring, [N,CO,C4<sup>-</sup>] and [N,CO,C3<sup>-</sup>] might also contribute, but these lie much higher in energy. In agreement with the work of Ohanessian and coworkers for the related (Zn+Gly-H)<sup>+</sup> complex, <sup>1-4</sup> we find that a plausible pathway for the rearrangement of the solution phase Zn<sup>+</sup>(Pro-H) to ZnH<sup>+</sup>(Pro-2H) can occur upon desolvation of the last solvent molecule.

**Acknowledgement.** We thank Aaron Chalifoux for helping to acquire the data. Financial support for this work was provided by the National Science Foundation, Grant CHE-2313553. We

gratefully acknowledge the *Nederlandse Organisatie voor Wetenschappellijk Onderzoek* (NWO) for the support of the FELIX Laboratory and a grant of computer time from the Center of High Performance Computing at the University of Utah.

**Supporting Information.** Comparison of  $Zn^+(Pro-H)(Pro)$  experimental IRMPD action spectrum with calculated IR spectra for R, $S[N,CO^-][N,CO]$  and S, $S[N,CO^-][N,CO]$  conformers. Reaction coordinate diagram for rearrangement of  $Zn^+(Pro-H)(H_2O)$  to  $ZnH^+(Pro-2H)$  along with structures and a table of their energies.

## References

- 1. Rogalewicz, F.; Hoppilliard, Y.; Ohanessian, G., Structures and fragmentations of zinc(II) complexes of amino acids in the gas phase. I. Electrosprayed ions which are structurally different from their liquid phase precursors. *Int. J. Mass Spectrom.* **2000**, *201*, 307-320.
- 2. Hoppilliard, Y.; Rogalewicz, F.; Ohanessian, G., Structures and fragmentations of zinc(II) complexes of amino acids in the gas phase. II. Decompositions of glycine–Zn(II) complexes. *Int. J. Mass Spectrom.* **2001**, *204*, 267-280.
- 3. Rogalewicz, F.; Hoppilliard, Y.; Ohanessian, G., Structures and fragmentations of zinc(II) complexes of amino acids in the gas phase. III. Rearrangement versus desolvation in the electrospray formation of the glycine-zinc complex. *Int. J. Mass Spectrom.* **2001**, *206*, 45-52.
- 4. Rogalewicz, F.; Hoppilliard, Y.; Ohanessian, G., Structures and fragmentations of zinc(II) complexes of amino acids in the gas phase: IV. Solvent effect on the structure of electrosprayed ions. *Int. J. Mass Spectrom.* **2003**, *227*, 439-451.
- 5. Boles, G. C.; Hightower, R. L.; Berden, G.; Oomens, J.; Armentrout, P. B., Zinc and Cadmium Complexation of l-Threonine: An Infrared Multiple Photon Dissociation Spectroscopy and Theoretical Study. *J. Phys. Chem. B* **2019**, *123*, 9343-9354.
- 6. Hofstetter, T. E.; Howder, C.; Berden, G.; Oomens, J.; Armentrout, P. B., Structural Elucidation of Biological and Toxicological Complexes: Investigation of Monomeric and Dimeric Complexes of Histidine with Multiply Charged Transition Metal (Zn and Cd) Cations using IR Action Spectroscopy. *J. Phys. Chem. B* **2011**, *115*, 12648-12661.
- 7. Boles, G. C.; Coates, R. A.; Berden, G.; Oomens, J.; Armentrout, P. B., Experimental and Theoretical Investigations of Infrared Multiple Photon Dissociation Spectra of Glutamine Complexes with Zn<sup>2+</sup> and Cd<sup>2+</sup>. *J. Phys. Chem. B* **2015**, *119*, 11607–11617.
- 8. Chalifoux, A. M.; Boles, G. C.; Berden, G.; Oomens, J.; Armentrout, P. B., Experimental and Theoretical Investigations of Infrared Multiple Photon Dissociation Spectra of Arginine Complexes with Zn<sup>2+</sup> and Cd<sup>2+</sup>. *Phys. Chem. Chem. Phys.* **2018**, *20*, 20712-20725.
- 9. Owen, C. J.; Boles, G. C.; Berden, G.; Oomens, J.; Armentrout, P. B., Experimental and Theoretical Investigations of Infrared Multiple Photon Dissociation Spectra of Lysine Complexes with Zn<sup>2+</sup> and Cd<sup>2+</sup>. Eur. J. Mass Spectrom. **2019**, 25, 97-111.

- 10. Boles, G. C.; Stevenson, B. C.; Hightower, R. L.; Berden, G.; Oomens, J.; Armentrout, P. B., Zinc and cadmium complexation of L-methionine: An infrared multiple photon dissociation spectroscopy and theoretical study. *J. Mass Spectrom.* **2021**, *56*, e4580.
- 11. Coates, R. A.; McNary, C. P.; Boles, G. C.; Berden, G.; Oomens, J.; Armentrout, P. B., Structural Characterization of Gas-Phase Cysteine and Cysteine Methyl Ester Complexes with Zinc and Cadmium Dications by Infrared Multiple Photon Dissociation Spectroscopy. *Phys. Chem. Chem. Phys.* **2015**, *17*, 25799-25808.
- 12. Coates, R. A.; Boles, G. C.; McNary, C. P.; Berden, G.; Oomens, J.; Armentrout, P. B., Zn<sup>2+</sup> and Cd<sup>2+</sup> Cationized Serine Complexes: Infrared Multiple Photon Dissociation Spectroscopy and Density Functional Theory Investigations. *Phys. Chem. Chem. Phys.* **2016**, *18*, 22434 22445.
- 13. Boles, G. C.; Owen, C. J.; Berden, G.; Oomens, J.; Armentrout, P. B., Experimental and Theoretical Investigations of Infrared Multiple Photon Dissociation Spectra of Glutamic Acid Complexes with Zn<sup>2+</sup> and Cd<sup>2+</sup>. *Phys. Chem. Chem. Phys.* **2017**, *19*, 12394 12406.
- 14. Boles, G. C.; Hightower, R. L.; Coates, R. A.; McNary, C. P.; Berden, G.; Oomens, J.; Armentrout, P. B., Experimental and Theoretical Investigations of Infrared Multiple Photon Dissociation Spectra of Aspartic Acid Complexes with Zn<sup>2+</sup> and Cd<sup>2+</sup>. *J. Phys. Chem. B* **2018**, *122*, 3836-3853.
- 15. Boles, G. C.; Coates, R. A.; Berden, G.; Oomens, J.; Armentrout, P. B., Experimental and Theoretical Investigations of Infrared Multiple Photon Dissociation Spectra of Asparagine Complexes with Zn<sup>2+</sup> and Cd<sup>2+</sup> and Their Deamidation Processes. *J. Phys. Chem. B* **2016**, *120*, 12486-12500.
- 16. Stevenson, B. C.; Martens, J.; Berden, G.; Oomens, J.; Armentrout, P. B., Spectroscopic Investigation of the Metal Coordination of the Aromatic Amino Acids with Zinc and Cadmium. *J. Phys. Chem. A* **2023**, *127*, 3560-3569.
- 17. Gholami, A.; Fridgen, T. D., Structures and Unimolecular Reactivity of Gas-Phase [Zn(Proline-H)]<sup>+</sup> and [Zn(Proline-H)(H<sub>2</sub>O)]<sup>+</sup>. J. Phys. Chem. B **2013**, 117, 8447-8456.
- 18. Gholami, A.; Fridgen, T. D., The unimolecular chemistry of [Zn(amino acid)<sub>2</sub>-H]<sup>+</sup> in the gas phase: H<sub>2</sub> elimination when the amino acid is a secondary amine. *Phys. Chem. Chem. Phys.* **2014**, *16*, 3134-3143.
- 19. Jami-Alahmadi, Y.; Fridgen, T. D., Structures and unimolecular chemistry of M(Pro<sub>2</sub>-H)<sup>+</sup> (M = Mg, Ca, Sr, Ba, Mn, Fe, Co, Ni, Cu, Zn) by IRMPD spectroscopy, SORI-CID, and theoretical studies. *Phys. Chem. Chem. Phys.* **2016**, *18*, 2023-2033.
- 20. Oepts, D.; van der Meer, A. F. G.; van Amersfoort, P. W., The Free-Electron-Laser User Facility FELIX. *Infrared Phys. Technol.* **1995**, *36*, 297-308.
- 21. Valle, J. J.; Eyler, J. R.; Oomens, J.; Moore, D. T.; van der Meer, A. F. G.; von Heldon, G.; Meijer, G.; Hendrickson, C. L.; Marshall, A. G.; Blakney, G. T., Free Electron Laser-Fourier Transform Ion Cyclotron Resonance Mass Spectrometry Facility for Obtaining Infrared Multiphoton Dissociation Spectra of Gaseous Ions. *Rev. Sci. Instrum.* **2005**, *76*, 023103.
- 22. Polfer, N. C.; Oomens, J.; Moore, D. T.; von Helden, G.; Meijer, G.; Dunbar, R. C., Infrared Spectroscopy of Phenylalanine Ag(I) and Zn(II) Complexes in the Gas Phase. *J. Am. Chem. Soc.* **2006**, *128*, 517-525.
- 23. Polfer, N. C.; Oomens, J., Reaction Products in Mass Spectrometry Elucidated with Infrared Spectroscopy. *Phys. Chem. Chem. Phys.* **2007**, *9*, 3804-3817.
- 24. Marshall, A. G.; Wang, T. C. L.; Ricca, T. L., Tailored Excitation for Fourier Transform Ion Cyclotron Resonance Mass Spectrometry. *J. Am. Chem. Soc.* **1985**, *107*, 7893-7897.

- 25. Guan, S. H.; Marshall, A. G., Stored Waveform Inverse Fourier Transform (SWIFT) Ion Excitation in Trapped-Ion Mass Spectrometry: Theory and Applications. *Int. J. Mass Spectrom. Ion Processes* **1996**, *158*, 5-37.
- 26. Dunbar, R. C., Infrared Radiative Cooling of Isolated Polyatomic Molecules. *J. Chem. Phys.* **1989**, *90*, 7369-7375.
- 27. Lemaire, J.; Boissel, P.; Heninger, M.; Mauclaire, G.; Bellec, G.; Hestdagh, H.; Simon, A.; Le Caer, S.; Ortega, J. M.; Glotin, F.; Maitre, P., Gas Phase Infrared Spectroscopy of Selectively Prepared Ions. *Phys. Rev. Lett.* **2002**, *89*, 273002-1 273002-4.
- 28. Frisch, M. J.; Trucks, G. W.; Schlegel, H. B.; Scuseria, G. E.; Robb, M. A.; Cheeseman, J. R.; Scalmani, G.; Barone, V.; Mennucci, B.; Petersson, G. A.; Nakatsuji, H.; Caricato, M. L., X.; Hratchian, H. P.; Izmaylov, A. F.; Bloino, J.; Zheng, G.; Sonnenberg, J. L.; Hada, M.; Ehara, M.; Toyota, K.; Fukuda, R.; Hasegawa, J.; Ishida, M.; Nakajima, T.; Honda, Y.; Kitao, O.; Nakai, H.; Vreven, T.; Montgomery, J. A., Jr.; Peralta, J. E.; Ogliaro, F.; Bearpark, M.; Heyd, J. J.; Brothers, E.; Kudin, K. N.; Staroverov, V. N.; Kobayashi, R.; Normand, J.; Raghavachari, K.; Rendell, A.; Burant, J. C.; Iyengar, S. S.; Tomasi, J.; Cossi, M.; Rega, N.; Millam, J. M.; Klene, M.; Knox, J. E.; Cross, J. B.; Bakken, V.; Adamo, C.; Jaramillo, J.; Gomperts, R.; Stratmann, R. E.; Yazyev, O.; Austin, A. J.; Cammi, R.; Pomelli, C.; Ochterski, J. W.; Martin, R. L.; Morokuma, K.; Zakrzewski, V. G.; Voth, G. A.; Salvador, P.; Dannenberg, J. J.; Dapprich, S.; Daniels, A. D.; Farkas, Ö.; Foresman, J. B.; Ortiz, J. V.; Cioslowski, J.; Fox, D. J.Gaussian 09, Revision D.01, Gaussian, Inc.; Wallingford CT, 2009. *Gaussian 09*, Revision D.01; Gaussian, Inc.: Wallingford CT, 2009.
- 29. Weigend, F.; Ahlrichs, R., Balanced Basis Sets of Split Valence, Triple Zeta Valence and Quadruple Zeta Valence Quality for H to Rn: Design and Assessment of Accuracy. *Phys. Chem. Phys.* **2005**, *7*, 3297-3305.
- 30. Andrae, D.; Haeussermann, U.; Dolg, M.; Stoll, H.; Preuss, H., Energy-adjusted Ab Initio Pseudopotentials for the Second and Third Row Transition Elements. *Theor. Chim. Acta* **1990,** 77, 123-141.
- 31. Feller, D., The Role of Databases in Support of Computational Chemistry Calculations. *J. Comput. Chem.* **1996**, *17*, 1571-1586.
- 32. Polfer, N. C., Infrared Multiple Photon Dissociation Spectroscopy of Trapped Ions. *Chem. Soc. Rev.* **2011**, *40*, 2211-2221.
- 33. Oomens, J.; Sartakov, B. G.; Meijer, G.; von Helden, G., Gas-Phase Infrared Multiple Photon Dissociation Spectroscopy of Mass-Selected Molecular Ions. *Int. J. Mass Spectrom.* **2006**, *254*, 1-19.
- 34. Heaton, A. L.; Bowman, V. N.; Oomens, J.; Steill, J. D.; Armentrout, P. B., Infrared Multiple Photon Dissociation Spectroscopy of Cationized Asparagine: Effects of Alkali-Metal Cation Size on Gas-Phase Conformation. *J. Phys. Chem. A* **2009**, *113*, 5519-5530.
- 35. Berglund, M.; Wieser, M. E., Isotopic Compositions of the Elements 2009. *Pure Appl. Chem.* **2011**, *83*, 397-410.
- 36. Boles, G. C.; Coates, R. A.; Berden, G.; Oomens, J.; Armentrout, P. B., Experimental and Theoretical Investigations of Infrared Multiple Photon Dissociation Spectra of Glutamine Complexes with Zn<sup>2+</sup> and Cd<sup>2+</sup>. *J. Phys. Chem. B* **2015**, *119*, 11607-11617.
- 37. Martens, J. K.; Grzetic, J.; Berden, G.; Oomens, J., Gas-phase conformations of small polyprolines and their fragment ions by IRMPD spectroscopy. *Int. J. Mass Spectrom.* **2015**, *377*, 179-187.

- 38. Shannon, R. D., Revised Effective Ionic Radii and Systematic Studies of Interatomic Distances in Halids and Chalcogenides. *Acta Crystallogr.* **1976**, *A32*, 751-767.
- 39. Georgiadis, R.; Armentrout, P. B., Kinetic Energy Dependence of the Reactions of Ca<sup>+</sup> and Zn<sup>+</sup> with H<sub>2</sub>, D<sub>2</sub>, and HD. Effect of Empty versus Full d Orbitals. *J. Phys. Chem* **1988**, *92*, 7060-7067.
- 40. Kapota, C.; Lemaire, J.; Maitre, P.; Ohanessian, G., Vibrational Signature of Charge Solvation vs Salt Bridge Isomers of Sodiated Amino Acids in the Gas Phase. *J. Am. Chem. Soc.* **2004**, *126*, 1836-1842.
- 41. Drayss, M. K.; Blunk, D.; Oomens, J.; Schäfer, M., Infrared Multiple Photon Dissociation Spectroscopy of Potassiated Proline. *J. Phys Chem. A* **2008**, *112*, 11972-11974.
- 42. Drayss, M. K.; Armentrout, P. B.; Oomens, J.; Schäfer, M., IR Spectroscopy of Cationized Aliphatic Amino Acids: Stability of Charge-solvated Structure Increases with Metal Cation Size. *Int. J. Mass Spectrom.* **2010**, *297*, 18–27.

# Table of Contents Graphic

